111690

aquifer/jdc/jof

Weldon Spring Site Remedial Action Project

Aquifer Characteristics Data Report for
The Weldon Spring Site Chemical Plant/Raffinate Pits
and Vicinity Properties

November 1990

Revision 0

DISCLAIMER

Prepared by

MK-FERGUSON COMPANY
and
JACOBS ENGINEERING GROUP
7295 Highway 94 South
St. Charles, Missouri 63303

Prepared for

U.S. DEPARTMENT OF ENERGY
Oak Ridge Operations Office
Under Contract DE-AC05-86OR21548

aquifer/jdc/jof

ABSTRACT

This report describes the procedures and methods used, and presents the results of physical testing performed, to characterize the hydraulic properties of the shallow Mississippian-Devonian aquifer beneath the Weldon Spring chemical plant, raffinate pits, and vicinity properties. The aquifer of concern is composed of saturated rocks of the Burlington-Keokuk Limestone which constitutes the upper portion of the Mississippian-Devonian aquifer. This aquifer is a heterogeneous anisotropic medium which can be described in terms of diffuse Darcian flow overlain by high porosity discrete flow zones and conduits. Average hydraulic conductivity for all wells tested is 9.6E-02 meters/day (3.1E-01 feet/day). High hydraulic conductivity values are representative of discrete flow in the fractured and weathered zones in the upper Burlington-Keokuk Limestone. They indicate heterogeneities within the Mississippian-Devonian aquifer. Aquifer heterogeneity in the horizontal plane is believed to be randomly distributed and is a function of fracture spacing, solution voids, and preglacial weathering phenomena. Relatively high hydraulic conductivities in deeper portions of the aquifer are thought to be due to the presence of widely spaced fractures.

Pumping tests conducted in the upper 12 meters (39 feet) of saturated bedrock provided values for transmissivity which ranged from 0.19 to 0.49 meters^2/day (15.5 to 39.9 gallons per day/foot). The average storativity determined from pumping tests is 4.9E-04. Results of pumping tests indicate a primary lateral anisotropy and poor hydraulic communication between pumped intervals and deeper portions of the Burlington-Keokuk Limestone. This suggests that appreciable upward leakage is unlikely from deeper portions of the aquifer to the test interval. Limited evidence of delayed yield may indicate double porosity effects.

Groundwater velocities average 1.1E-01 meters/day (3.6E-01 feet/day). Calculated groundwater velocities and travel times are consistent with observed contaminant distribution, although actual flowpaths are expected to exhibit nonlinear aspects resulting in significant variations in velocity.

Pumping and tracer tests did not intercept free flow zones, or conduits capable of supplying sustained pumpage in excess of 1.5 liters/minute (0.4 gallons/minute). However, slug testing indicates the existence of randomly distributed high porosity zones in the upper saturated portion of the formation. Additional pumping tests in these locations would provide information on discrete flow properties.

TABLE OF CONTENTS

TABLE OF CONTENTS

TABLE OF CONTENTS

LIST OF FIGURES

LIST OF FIGURES

LIST OF TABLES

1 INTRODUCTION

This Aquifer Characteristics Data Report (ACDR) presents the results of investigations designed to physically characterize the hydrogeologic regime of the uppermost bedrock formation beneath the Weldon Spring Site chemical plant, raffinate pits, and vicinity properties (WSCP/RP/VP). Specifically, this report presents the results of slug tests and pumping and tracer testing. Slug tests and pumping tests were conducted as elements of hydrogeologic investigations sampling (MKF and JEG 1988b). Tracer tests were performed to complement physical aquifer characterization with respect to effective porosity and dispersivity.

The ACDR constitutes a portion of the Weldon Spring Site Remedial Action Project (WSSRAP) characterization program designed to support the Remedial Investigation/Feasibility Study (RI/FS) under the Comprehensive Environmental Response, Compensation and Liability Act (CERCLA).

1.1 Site Description

The chemical plant and raffinate pits are is located in St. Charles County, Missouri, approximately 48 km (30 mi) west of St. Louis and 23 km (14 mi) southwest of St. Charles as shown in Figure 1-1. The site is situated on Missouri State Highway 94 about 3 km (2 mi) southwest of the junction of Highway 94 with U.S. Routes 40 and 61. The site is surrounded by State and Federally owned lands. It is adjoined on the west by the Weldon Spring Training Area (WSTA) and on the east, north, and south by Missouri Department of Conservation (MDOC) lands.

MISSISSIPPI RIVER

MISSOURI RIVER

ST. LOUIS

O'FALLON

ST. CHARLES

ST. PETERS

WELDON SPRING

WELDON SPRING
CHEMICAL PLANT/
RAFFINATE PITS

WELDON SPRING
QUARRY

MISSOURI RIVER

MERAMEC RIVER

SCALE   MILES

0   4   8
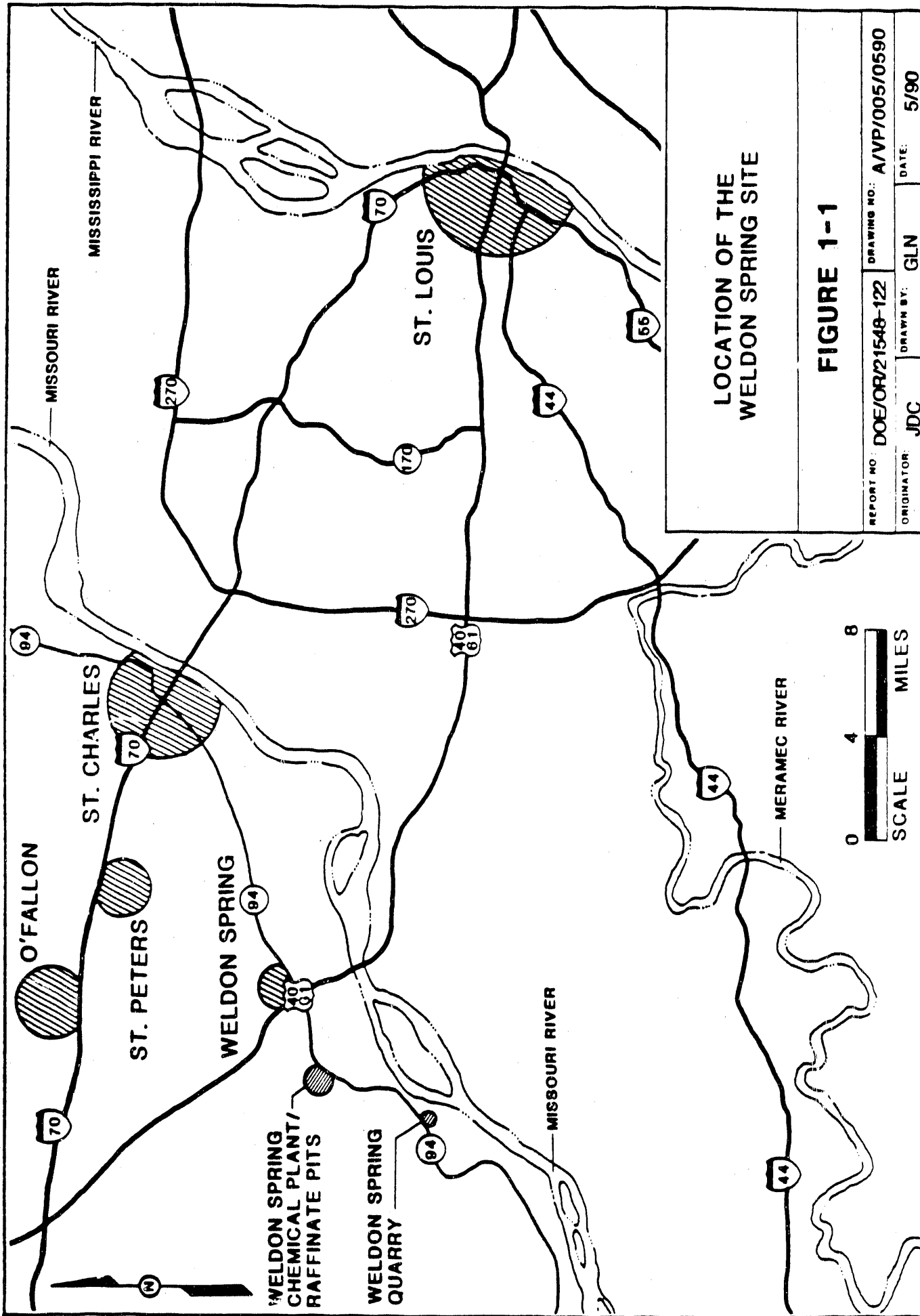
LOCATION OF THE
WELDON SPRING SITE

FIGURE 1-1

REPORT NO: DOE/OR/21548-122   DRAWING NO: A/VP/005/0590

ORIGINATOR: JDC   DRAWN BY: GLN   DATE: 5/90

The community of Weldon Spring, with a population of approximately 700, is located approximately 3 km (2 mi) north of the Weldon Spring site (WSS). The metropolitan area of St. Louis, with a population exceeding 2.5 million, is within 48 km (30 mi) of the site.

1.2 Site History

The site history, including previous decontamination efforts from 1941 to 1987, is summarized below. A more detailed history of WSS operations is included in the WSSRAP Remedial Investigation/Feasibility Study Work Plan (ORNL 1988).

The land encompassing the WSS was privately held until April 1941 when the Department of the Army (DA) acquired 6,974 ha (17,232 ac) of land. From November 1941 through January 1944, Atlas Powder Company operated a trinitrotoluene (TNT) and dinitrotoluene (DNT) explosives production facility known as the Weldon Spring Ordnance Works (WSOW). After another production operation during 1945 and 1946 the WSOW was closed in April 1946 and declared surplus to Army needs. By 1949, all but approximately 809 ha (2,000 ac) had been transferred back to the State of Missouri (August A. Busch Memorial Wildlife Area) and the University of Missouri (agricultural land). Except for several small parcels of land transferred to St. Charles County, the remaining property became the WSTA.

Through a Memorandum of Understanding between the Secretary of the Army and the Atomic Energy Commission (AEC) in May 1955, 83 ha (205 ac) of the former WSOW were transferred to the AEC for the construction and operation of the Weldon Spring Uranium Feed Materials Plant (WSUFMP) to process uranium and thorium ore

concentrates. The DA decontaminated a considerable portion of the WSOW before construction of the WSUFMP commenced (DA 1976).

The WSUFMP processed uranium and thorium ore concentrates from 1957 to 1966 with the Uranium Division of Mallinckrodt Chemical Works acting as the AEC operating contractor. This facility consisted of 13 major process buildings and approximately 30 support structures. The AEC closed the WSUFMP in December 1966.

On August 7, 1967, approximately 67 ha (166 ac) of the AEC facility were selected as the site for a herbicide production facility, later known as the Weldon Spring chemical plant (WSCP). The remaining 21-ha (51-ac) area, encompassing four process waste lagoons called the Weldon Spring raffinate pits (WSRP), remained under AEC control. Figure 1-2 is a site plan of the WSCP and WSRP. On December 31, 1967, 67 ha (166 ac) of property and improvements were transferred to the Kansas City District, U.S. Army Corps of Engineers, which was responsible for the design and construction of the herbicide facility.

Decontamination and dismantling operations were initiated in January 1968. Some progress was made in the decontamination of areas required for herbicide production equipment before the project was cancelled in February 1969. This cancellation was due in part to costs required to comply with the radiological contamination limits imposed on the facility and in part to a reduction of the DA's requirements for herbicide.

The herbicide project was cancelled before any production equipment was installed. However, the DA retained responsibility for the land and facilities at the WSCP.

DOE PROPERTY FENCE

FROG POND

DOE PROPERTY FENCE

WSCP

ASH POND

RAFFINATE PIT NO.4

RAFFINATE PIT NO.3

RAFFINATE PIT NO.1

WSRP

RAFFINATE PIT NO.2

DOE PROPERTY FENCE

N

MAGNETIC NORTH

TRUE NORTH

| 0 | 500' | 1000' |

SCALE

MAP OF THE WSCP & WSRP		
FIGURE 1-2		
REPORT NO.: DOE/OR/21548-122	DRAWING NO.: A/CP/003/0590	
ORIGINATOR: JDC	DRAWN BY: GLN	DATE: 5/90
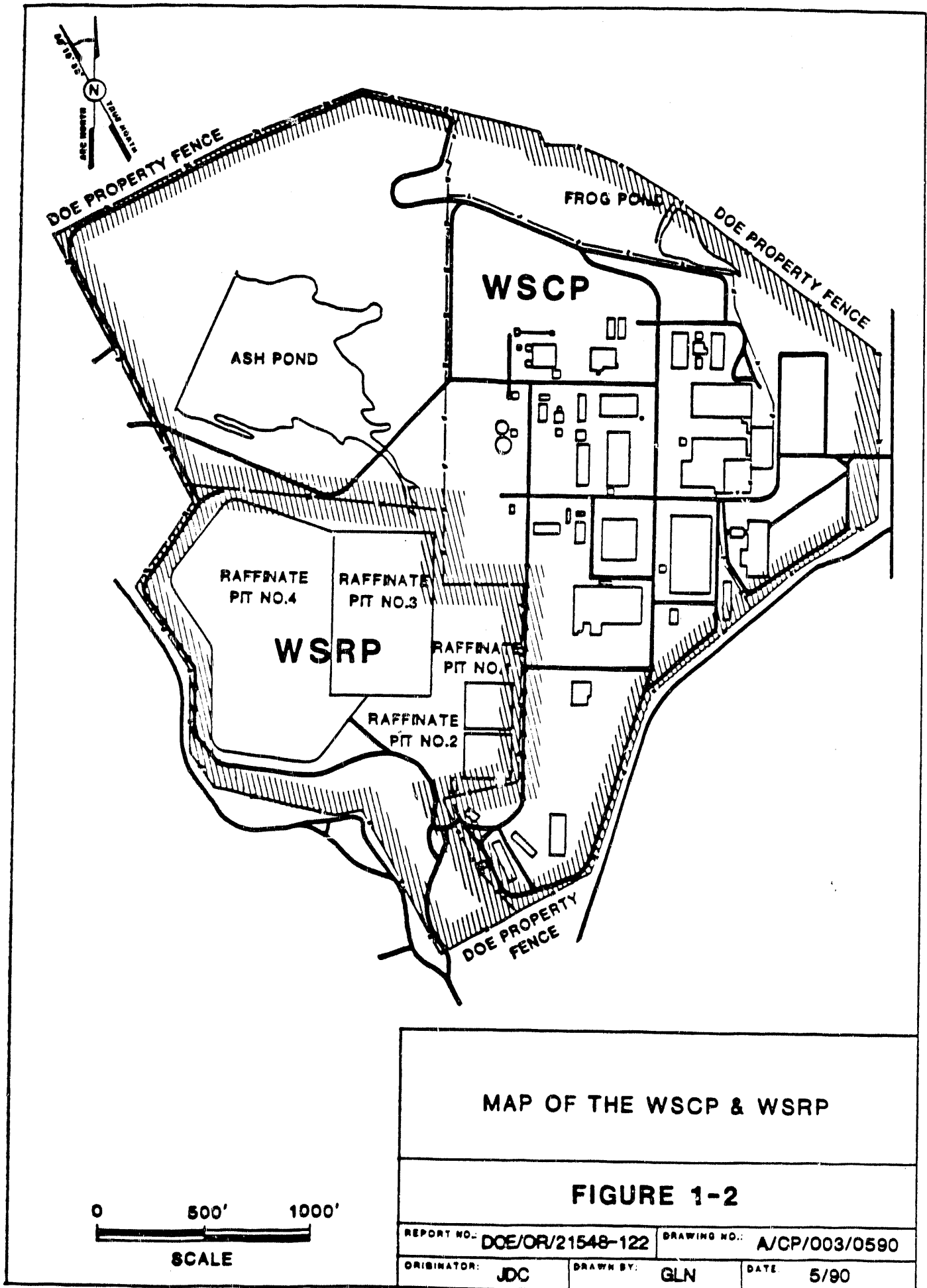
The AEC contracted with National Lead Company of Ohio (NLO) to visit the WSRP periodically for environmental monitoring and to maintain the pit embankments and perform maintenance and surveillance tasks as necessary. Bechtel National, Inc. (BNI) assumed management responsibility for the WSRP from NLO in October 1981 under contract to the U.S. Department of Energy (DOE) which succeeded the AEC.

In November 1984, the U.S. Department of Energy (DOE) was directed by the Office of Management and Budget to assume custody and accountability for the WSCP from the DA. This transfer occurred on October 1, 1985.

In February 1985, the DOE proposed designating control and decontamination of the WSS as a major project. Designation was effected by DOE Order 4240.1E dated May 14, 1985. A Project Management Contractor (PMC) for the WSSRAP was selected in February 1986. In July 1986, a DOE Project Office was established on site. The PMC, MK-Ferguson Company, assumed control of the WSS on October 1, 1986.

2 GEOLOGIC SETTING

This section presents background information on the regional and local geology based on information available from published reports, results of previous investigations, and data derived from Project Management Contractor (PMC) investigations.

2.1 Regional Physiography and Geology

The site lies at the southern edge of the dissected till plains of the Central Lowlands Physiographic Province, which is characterized by gently rolling hills in upland areas (ORNL 1988). South of the site, the topography changes dramatically as the dissected till plains give way to narrow ridges and valleys which characterize the Ozark Plateau Physiographic Province. The surface drainage divide between the Mississippi River to the north and the Missouri River to the south bisects the site from southwest to northeast.

The stratigraphy in the Weldon Spring area is composed of approximately 610 to 915 m (2,000 to 3,000 ft) of Paleozoic Era marine limestone, dolomite, sandstone, and shale. A detailed description of regional stratigraphy is given by BNI (1987) and MKF and JEG (1989b). The bedrock in the Weldon Spring area exhibits a regional strike of N601°W and a regional dip of approximately 1° to the northeast. Due to vertical crustal movements during the Paleozoic Era, rocks of the Central Stable Region, of which Missouri is a part, were deformed into broad basins and arches (Eardley 1951). The closest of these features, the northwest trending House Springs-Eureka anticline, is located about 6 km (4 mi) southwest of the site. The rocks on the northeast limb of the fold strike approximately N60°W and dip approximately 0.5° to 1° to the northeast.

Geologic mapping of the Weldon Spring 7.5-minute quadrangle by the Missouri Department of Natural Resources Division of Geology and Land Survey (MDNR-DGLS) shows an east-west trending normal fault located approximately 1.6 km (1 mile) north of the site. The fault is reported to display approximately 18 m (60 ft) of vertical displacement with the north block down (Whitfield et al. 1989).

2.2 Geology of the Weldon Spring Chemical Plant, Raffinate Pits, and Vicinity Properties

The Weldon Spring Chemical Plant/Raffinate Pits/Vicinity Properties (WSCP/RP/VP) extend over several distinct geologic units that are pertinent to this study. There are several distinguishable overburden units and two units in the uppermost bedrock. The following subsections describe the principal geologic units based on information contained in the Geologic Report on Weldon Spring Raffinate Pits Site (BNI 1984), Hydrogeological Characterization Report for Weldon Spring Chemical Plant (BNI 1987), and the Draft Remedial Investigation Report (MK-F and JEG 1989b).

2.2.1 Geology of Unconsolidated Material

Unconsolidated surficial materials at the site are composed of fill material, loess, interglacial sediment, glacial tills, and residuum. The thickness of the surficial units ranges from 5 to 18 m (15 to 60 ft) and is controlled both by surface erosional features and bedrock topography. The unconsolidated units are generally thickest in the north central portion and thinnest in the eastern third of the site. The unconsolidated materials have been divided into six distinguishable units based on physical

characteristics observed during sampling and laboratory testing
(MK-F and JEG 1989b).

2.2.1.1 Topsoil/Fill

The uppermost soil unit is composed of topsoil or fill
material. This unit ranges up to 9 m (30 ft) in thickness. The
topsoil fraction is widespread on site and ranges up to 1 m
(3.5 ft) in thickness. It is generally a black, organically rich
clayey-silt to silty-clay. The fill portion of the unit varies
greatly in thickness because of its use as construction material
for the raffinate pit dikes and Ash Pond dike, and recontouring
of low areas prior to construction of buildings. The fill
composition varies but is primarily clayey silt which is believed
to have originated on or near the site.

2.2.1.2 Loess

Underlying the topsoil/fill unit is an upper Pleistocene
loess unit that is distributed sporadically on the site due to
pre-depositional topography, post-depositional erosion, and
extensive reworking of site soils during site preparation and
construction. Subsurface data indicate that the loess ranges up
to 3 m (10 ft) in thickness. The unit is a low plasticity silt
to clayey silt with very minor amounts of sand.

2.2.1.3 Ferrelview Formation

A mid-Pleistocene interglacial sediment interpreted as being
the Ferrelview Formation underlies the loess and is present
across most of the site. The Ferrelview is described in detail
by Howe and Heim (1968). The unit ranges up to 6.5 m (22 ft) in
thickness and consists of a mottled gray and dark yellowish-

orange silty-clay to clayey-silt. The unit is generally stiff
and plastic. Iron oxide nodules and manganese oxide (pyrolusite)
precipitates are common. The unit commonly displays slickensides
as a result of post-depositional compaction and consolidation.
Also, irregular blocky fractures are sometimes encountered which
continue through the underlying clay till. Blocky fractures are
described as tight dry features which are often coated with
calcium or manganese minerals of a powdery or concretionary
nature. Laboratory tests for particle size distribution indicate
mostly silt- and clay-sized particles in this unit with minor
sand and fine gravel (MK-F and JEG 1989b).

2.2.1.4 Clay Till

The clay till unit is a lower Pleistocene glacial till which
underlies the Ferrelview Formation and is the most areally
extensive overburden unit on the site. The clay till ranges in
thickness to 9 m (30 ft) and is found in almost all boreholes and
trenches on site. This unit is composed of yellowish-brown
silty-clay and clayey-silt with some sand and rounded pebbles of
chert and igneous and metamorphic detritus. Material in this
unit is very stiff and moderately to highly plastic. Blocky
fractures coated with pyrolusite are abundant.

2.2.1.5 Basal Till

The basal till unit is the lowest member of the Pleistocene
glacial till sediments found on the site. It underlies the clay
till and is found mainly on the western and north central
portions of the site. Deposition of the basal till unit may have
been influenced by bedrock topography since the unit is generally
thin or absent in areas of higher bedrock elevations, and is
thicker where bedrock elevations are lower. The basal till

ranges in thickness up to 3 m (10 ft) and can generally be described as a yellowish-brown sandy, clayey, silty-gravel with angular chert in a poorly bound matrix.

2.2.1.6 Residuum

The residuum unit is located beneath the basal till and clay till unit where the basal till is absent. The residuum forms the base of the unconsolidated material and is interpreted to be a pre-Pleistocene weathering product of the underlying cherty argillaceous limestone. The unit varies in thickness up to 8 m (26 ft) and is highly heterogeneous, ranging from a typically gravel dominated matrix to a gravelly-clay to gravelly-silt. The gravel fraction is generally weathered chert fragments but also consists of minor weathered limestone. Sample recovery in this unit is very difficult due to the large gravel fraction. As such, the unit is hard to characterize without using in situ methods.

2.2.2 Bedrock Geology

The uppermost bedrock unit at the Weldon Spring site (WSS) is the Burlington- Keokuk Limestone. This is a fine- to coarse-grained, thinly to massively bedded argillaceous to crystalline limestone containing abundant chert as nodules and beds. From borehole stratigraphic data, the formation has been divided into two units based primarily on weathering characteristics. The upper division is referred to as the weathered limestone portion, and the lower division is referred to as the competent limestone.

Roberts (1951) reported two major joint sets present within the exposed bedrock in the Weldon Spring area; one set trends between N30°W and N65°W and the other set trends N30°E to N72°E.

Subsequent regional and site-specific joint studies have generally confirmed these orientations (BGA 1984, MK-F and JEG 1987 and 1988b). Bedrock topography exhibits erosional features interpreted as paleochannels, which coincide with observed joint set orientations (MKF and JEG 1989b). Additionally, present-day drainages within the Missouri River watershed are incised into bedrock and exhibit strong linearity coincident with joint set trends. Drainage trends within the Mississippi River watershed are more sinuous than those in the Missouri River watershed and do not exhibit linearity due to the presence of overlying, unconsolidated sediments.

2.2.2.1 Weathered Limestone

The weathered limestone ranges in thickness from 3 to greater than 15 m (10 to greater than 50 ft), and is typically a grayish-orange to yellowish gray, argillaceous limestone, commonly containing as much as 60% chert as nodules and interbeds. Minor interbeds of fossiliferous, finely crystalline limestone occur near the top of the unit in some cores. The unit is moderately to highly fractured, slightly to severely weathered, with abundant iron oxide staining and manganese oxide in the rock matrix and along fractures. Solution features are quite common in this unit, ranging from pinpoint vugs to small cavities up to 1.5 m (5 ft) in diameter (BNI 1987). Many of the smaller vugs are lined with calcite and drusy to euhedral quartz. The larger cavities in many cases appear to be at least partially filled with clay or silt/clay/chert/gravel mixtures. These cavities are generally reported as core loss in the boring logs. In some locations, recognition of top of bedrock was hindered due to alternating rock and clay-rich zones at or near the bedrock surface. Rock quality designations (RQD) are generally poor to very poor indicating a high degree of fracturing and/or

weathering. Core samples from angled boreholes indicate that fracturing in the weathered limestone is predominantly horizontal and loosely spaced, typically occurring along shaley interbeds, bedding planes, or chert interbeds (MK-F and JEG 1990b). Mineralization and clay deposition along fractures is common.

2.2.2.2 Competent Limestone

Underlying the weathered portion of the Burlington-Keokuk Limestone is the competent limestone, which is thinly to massively bedded, gray to light gray, finely to coarsely crystalline, stylolitic, and fossiliferous. The rock is slightly weathered to fresh, containing 20% to 40% chert. Cored material shows very little iron oxide staining and exhibits unaltered pyrite on some fracture surfaces. Both horizontal and vertical fracture densities are significantly lower in the competent limestone than in the weathered limestone (MK-F and JEG 1990b).

3 HYDROGEOLOGIC SETTING

This section presents background information on regional and local hydrogeology based on information available from published reports, results of previous investigations, and Project Management Contractor (PMC) derived data.

3.1 REGIONAL HYDROGEOLOGY

Three principal aquifer systems have been identified in the Weldon Spring area. These are the alluvial aquifers, the shallow bedrock aquifer system, and the deep bedrock aquifer system. Additionally, a leaky confining unit is recognized (Kleeschulte and Emmett 1987).

The major alluvial aquifers in western St. Charles County consist of saturated sands, gravels, and silts which compose the alluvium of the Missouri River and Mississippi River floodplains (Kleeschulte and Emmett 1986). Yields to wells from these aquifers range up to 9,800 lpm (2,600 gpm) along the major rivers (BNI 1987). Recharge to the alluvial aquifers occurs from infiltration of precipitation, increases in bank storage due to flooding, and as underflow in the form of regional discharge from bedrock aquifers. Fluvial recharge may also be induced in some locations due to pumping of large-capacity wells near the Missouri River (Kleeschulte and Emmett 1986).

The shallow bedrock aquifer system is composed of saturated Mississippian and Devonian aged rocks which range from 76 to 197 m (250 to 650 ft) in thickness and compose the uppermost bedrock units in the area. These units correspond to the Mississippian-Devonian aquifer system as depicted in Figure 3-1.

SYSTEM	SERIES	STRATIGRAPHIC UNIT	TYPICAL THICKNESS (ft)	LITHOLOGY	HYDROSTRATIGRAPHIC UNIT
QUARTERNARY	HOLOCENE	ALLUVIUM	0.5-4		ALLUVIAL AQUIFER
	PLEISTOCENE	LOESS, GLACIAL TILL, INTERGLACIAL SEDIMENT AND RESIDUUM	15-55		(unsaturated). *
MISSISSIPPIAN	MERAMECIAN	SALEM FORMATION	0-15		(unsaturated) . *
		WARSAW FORMATION	60-80		MISSISSIPPIAN-DEVONIAN ACUIFER SYSTEM
	OSAGEAN	BURLINGTON-KEOKUK LIMESTONE	100-200		
		FERN GLEN FORMATION	45-70		
	KINDERHOOKIAN	CHOUTEAU GROUP	20-50		
		BUSHBERG SANDSTONE	5-20		
DEVONIAN	UPPER	LOWER SULPHUR SPRINGS GROUP (UNDIF)	0-2		
	CINCINNATIAN	MAQUOKETA SHALE	10-30		ORDOVICIAN LEAKY CONFINING UNIT
		KIMMSWICK LIMESTONE	70-100		
		DECORAH GROUP	30-60		
	CHAMPLAINIAN	PLATTIN LIMESTONE	100-130		
		JOACHIM DOLOMITE	80-105		
ORDOVICIAN		ST. PETER SANDSTONE	120-150		
		POWELL DOLOMITE	50-60		ORDOVICIAN-CAMBRIAN AQUIFER SYSTEM
		COTTER DOLOMITE	200-250		
	CANADIAN	JEFFERSON CITY DOLOMITE	180-180		
		ROUBIDOUX FORMATION	150-170		
		GASCONADE DOLOMITE	250		
CAMBRIAN	UPPER	EMINENCE DOLOMITE	290		
		POTOSI DOLOMITE	100		

* THESE UNITS ARE BELIEVED TO BE UNSATURATED IN THE WSS VICINITY

MODIFIED FROM : MKF & JEG, 1989; WHITFIELD ET. AL. 1989; KLEESHULTE AND EMMETT, 1987

GENERAL STRATIGRAPHY AND HYDROSTRATIGRAPHY OF THE WELDON SPRING AREA

FIGURE 3-1

REPORT NO DOE/OR/21548-122	EDHIBT NO: A/PI/075/1190
ORIGINATOR JDC	DRAWN BY GLN	DATE 11/90

In the Weldon Spring area the Mississippian-Devonian aquifer system includes formations from the Burlington-Keokuk Limestone through the lower part of the Sulphur Springs Group. Reported yields to wells from this aquifer range from less than 4 lpm to 190 lpm (1 gpm to 50 gpm) (BNI 1987), but typically are from 19 lpm to 55 lpm (5 to 15 gpm). The higher yield wells are those that intercept zones of extensive secondary porosity such as joints and solution openings. The Mississippian-Devonian aquifer system is recharged by direct infiltration of precipitation along fractures and bedding planes in outcrop areas, unsaturated flow through unconsolidated overburden, and losing stretches of streams encounter bedrock joints. Discharge occurs as springs, seeps, evapotranspiration, underflow to the deeper portions of the bedrock under downward hydraulic gradient conditions, and as water supply wells are pumped (Kleeschulte and Emmett 1986).

Examination of potentiometric data from the Weldon Spring area by Kleeschulte and Emmett (1987) indicates that a groundwater divide runs beneath the trend of the ridge which divides surface water drainage between the Missouri and Mississippi watersheds.

A leaky confining layer is present below the Mississippian-Devonian aquifer from the top of the Maquoketa Shale down through the Joachim Dolomite. These units correspond to the Ordovician leaky confining unit as depicted in Figure 3-1. Individual units or zones within the leaky confining layer may yield low to moderate amounts, 40 to 190 lpm (10 to 50 gpm), of potable water on a local basis. The confining sequence is approximately 121 m (400 ft) thick (Kleeschulte and Emmett 1986).

The Ordovician-Cambrian aquifer system is approximately
305 m (1,000 ft) thick and consists of Ordovician and Upper
Cambrian formations, which include the St. Peter Sandstone
through the Potosi Dolomite (Kleeschulte and Emmett 1987). These
units correspond to the Ordovician-Cambrian aquifer system as
depicted in Figure 3-1. Yields from this aquifer range from 40
to 1900 lpm (10 to 500 gpm) (BNI 1987). Recharge to the
Ordovician-Cambrian aquifer occurs primarily as direct
infiltration of precipitation where the Ordovician units outcrop
southwest of the Weldon Spring area. Additionally, recharge
occurs where losing stretches of streams penetrate the aquifer
near the outcrop area, and as underflow from superjacent aquifers
under conditions of downward hydraulic gradient. Discharge from
the Ordovician-Cambrian aquifer occurs principally as underflow
to the alluvial and Mississippian-Devonian aquifers under upward
hydraulic gradient conditions, and as evapotranspiration and
seepage to springs and streams where the aquifer crops out.

3.2 Hydrogeology of the Weldon Spring Chemical Plant/Raffinate Pits/Vicinity Properties

The following subsections provide background information
about the hydrogeologic regime at the Weldon Spring site (WSS)
based on information available from previous investigations.

3.2.1 Surface Water/Groundwater Interaction

Spring and seep surveys, seepage runs, and dye trace and
water trace studies have been conducted in the area around the
WSS by the Missouri Department of Natural Resources (MDNR) and
U.S. Geological Survey (USGS).

The locations of known springs and seeps within various
tributary drainage basins are shown on Figure 3-2. Springs in
the vicinity of the site vary from small seeps at bedrock and
clay interfaces to solution enlarged bedrock conduits and
fractures having flow rates of 750 lpm (200 gpm) or more during
precipitation events. Some of the springs are wet weather
springs, flowing only in response to significant rainfall events.
Wet weather flow may be quite heavy, but is usually of short
duration (MKF and JEG 1988b).

Several tributaries around the WSS have losing segments
which have been identified by the MDNR (Dean 1983, 1984a, 1984b,
and 1985) and the USGS (Kleeschulte and Emmett 1986; Kleeschulte
et al. 1986). The results of dye trace studies conducted by the
MDNR in the 6000-series drainages (Mississippi River Basin)
indicate a probable subsurface connection between the unnamed
tributary of Schote Creek that drains Ash Pond and the raffinate
pit areas and the Burgermeister Spring area. Results of dye
trace studies conducted by the MDNR in the 5000-series drainages
(Missouri River Basin) indicate that a groundwater divide exists
north of the area, and water lost to the streambed in the
southeast drainage easement stays within the drainage boundary.
Furthermore, at least some of the flow lost in the upper reaches
of the southeast drainage easement re-emerges through springs in
the lower reaches (MDNR 1989).

3.2.2 Unconsolidated Materials

The unconsolidated materials at the site are, for the most
part, unsaturated. Unsaturated flow is present locally as a
result of direct infiltration, leakage from on-site storm water,
sewer and water lines, and leakage from the raffinate pits.
Saturated conditions also exist due to mounded and perched

SPRINGS AND SEEPS IN THE
WELDON SPRING AREA

FIGURE 3-2

REPORT NO DOE/OR/21548-122   EXHIBIT NO A/VP/053/1190
ORIGINATOR JDC   DRAWN BY GLN   DATE 11/90

groundwater. Mounded conditions are apparent beneath the
raffinate pits due to leakage. Perched conditions occur where
leakage or infiltration accumulates over low permeability clay-
rich horizons and in discrete permeable lenses.

Hydraulic conductivities and moisture content values of
unconsolidated materials as determined by laboratory methods are
presented in the site Remedial Investigation (RI) report (MKF and
JEG 1989b). The saturated hydraulic conductivity values are
generally quite low. Slug tests were performed by the PMC in
March 1987 on wells that monitor seasonally saturated portions of
the clay till unit in the vicinity of the raffinate pits. The
results of these tests indicate an average saturated hydraulic
conductivity of 1.0E-05 m/d (3.4E-05 ft/d) for the clay till unit
(Allan 1987). This value agrees well with laboratory test
results presented in the site RI report (MKF and JEG 1989b).

Ten lysimeters are currently in place at three locations
around the perimeter of the raffinate pits. The locations of the
lysimeters are indicated in Figure 3-3. Lysimeters LY-3604, LY-
3605, LY-3606, and LY-3607, located north of Raffinate Pit 3,
monitor silty zones over clay layers. Soil moisture from this
location is considered to be leakage from Raffinate Pit 3 due to
the elevated concentrations of nitrate, sulfate, and total
uranium detected in samples from that location. Lysimeters LY-
3608, LY-3609, and LY-3610 are located near the northwest corner
of Raffinate Pit 1. Lysimeter LY-3609 and LY-3610 have not
detected any moisture since installation, although they maintain
a vacuum. A sample taken from LY-3608 indicates that near
surface moisture (1.7 m (6 ft) below ground surface) is leakage
from Raffinate Pit 1 due to the high concentration of nitrate.
Lysimeters LY-3601, LY-3502, and LY-3603 are located at the base
of the west berm of Raffinate Pit 4 near a small seep. Analysis

DOE PROPERTY FENCE

FROG POND

DOE PROPERTY FENCE

ASH POND

LY3604
LY3605
LY3606
LY3607

RAFFINATE
PIT NO.4

RAFFINATE
PIT NO.3

RAFFINATE
PIT NO.1

LY3601
LY3602
LY3603

RAFFINATE
PIT NO.2

LY3608
LY3609
LY3610

DOE PROPERTY
FENCE
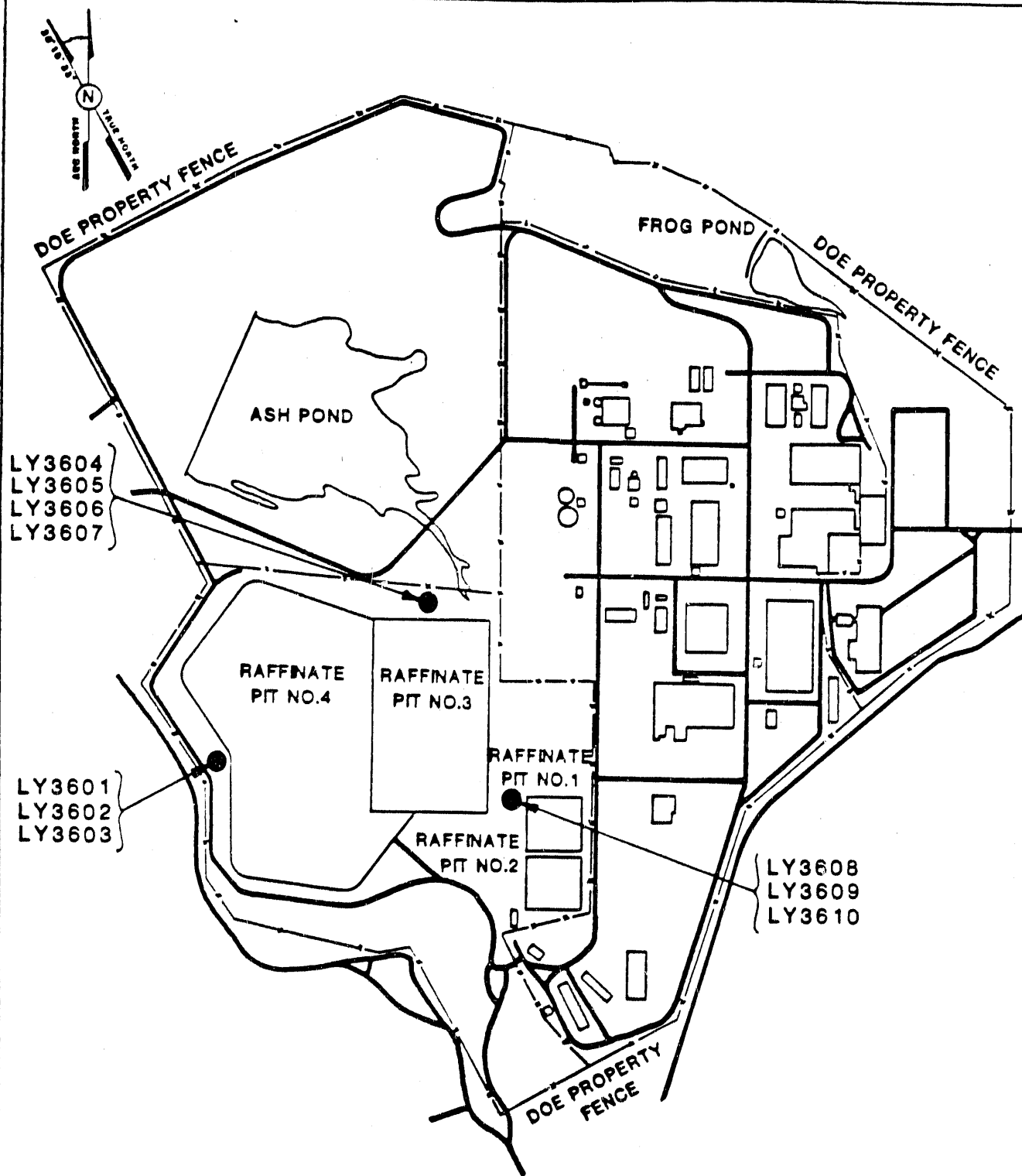
LOCATIONS OF LYSIMETERS AT
THE WELDON SPRING SITE

FIGURE 3-3

SCALE			
REPORT NO. DOE/OR/21548-122		DRAWING NO. A/CP/095/1190	
ORIGINATOR JDC	DRAWN BY GLN	DATE 11/90	

SCALE
0   500   1000 FT
0   152.4   304.8 M

of the seep water and soil moisture suggest that this seep is a
local discharge for infiltration which is captured by the riprap
on the west flank of the west berm of Raffinate Pit 4.

Previous exploratory drilling investigations at the WSS
indicated areas of anomalously high groundwater elevations or
perched groundwater in the vicinity of the raffinate pits (BGA
1984; BNI 1984; and UNC Geotech 1988). Details regarding
monitoring efforts designed to characterize saturated conditions
in the surficial soils are given in the site RI report.

Seismic refraction surveys performed by Weston Geophysical
Corporation (BNI 1984) detected velocity zones of 1,515 m/s
(5,000 ft/s) in the vicinity of Raffinate Pit 3 which may be
indicative of saturated conditions. The geophysical data
indicate that the subsurface soil beneath Raffinate Pit 3 may be
saturated and that saturated soil may also be present beneath
unsaturated materials on the east, west, and south sides of
Raffinate Pit 3. Subsequent borings in the vicinity of the
raffinate pits have confirmed that localized saturated conditions
are present (MKF and JEG 1989b).

3.2.3 Mississippian-Devonian Aquifer System

The Mississippian-Devonian aquifer system is the uppermost
aquifer present in the vicinity of the WSS. The upper portion of
the aquifer consists of saturated rocks of the Burlington-Keokuk
Limestone. As described in Section 3.1, this unit is subdivided
on the basis of weathering in the vicinity of the site. At the
WSS the lowermost unit in the Mississippian- Devonian aquifer
system is the Bushberg Sandstone. Groundwater flow in the
vicinity of the site is characterized by Darcian diffuse flow
with conduit flow superimposed. The dynamics of groundwater flow

through the upper portion of the Mississippian-Devonian aquifer
can best be described in terms of hydraulic head distribution.
That is, groundwater flows from areas of high hydraulic head to
areas of lower hydraulic head. Darcian principles may be applied
to assess flow characteristics on a scale much larger than that
of the spacing of individual fractures that have not been
significantly enlarged by dissolution. Specific conduit flow
pathways in the vicinity of the site have been defined from dye
injection and water tracing performed by the MDNR (MDNR 1989).

Potentiometric data indicate the presence of a groundwater
divide trending from the southwestern to northeastern portions of
the site. Figure 3-4 is a potentiometric surface map based on
data collected in December 1988 from shallow groundwater
monitoring wells. Groundwater to the north of this divide flows
northerly toward Dardenne Creek and groundwater to the south of
the divide flows southerly toward the Missouri River.

Borehole packer testing of the saturated bedrock has
revealed a general decrease in hydraulic conductivity with depth.
Water quality data from the Weldon Spring chemical plant/
raffinate pits/vicinity properties (WSCP/RP/VP) monitoring well
network indicate that although a downward hydraulic gradient
exists between the shallower and deeper monitoring wells, the
degree of communication is very limited (MKF and JEG 1989a).
Contaminants detected in wells monitoring the shallower portion
of the aquifer are generally present at lower concentrations or
not at all in deeper monitoring wells. Vertical hydraulic
conductivity is considered to be a function of vertical fracture
spacing. Angle hole drilling indicates thatspacing of vertical
fractures is sporadic, ranging from 0.75 m (2.5 ft) to 5.5 m
(18 ft), and averages 3 m (10 ft). The ratio of horizontal to

GROUNDWATER DIVIDE

FROG POND

ASH POND

RAFFINATE PIT NO.1

RAFFINATE PIT NO.2

RAFFINATE PIT NO.3

RAFFINATE PIT NO.4

590
585
580
575
570
565
560
555
550
570
575
580
585
590
560
565
600
605
610
605
610
600
585
595

TRUE NORTH
AGC NORTH
N
26° 10' 33"

SCALE

| 0 | 500 | 1000 FEET |
| 0 | 152.4 | 304.8 METERS |

REPORT NO.: DOE/OR/21548-122   DRAWING NO.: A/CP/004/0590

ORIGINATOR: JDC   DRAWN BY: GLN   DATE: 5/90
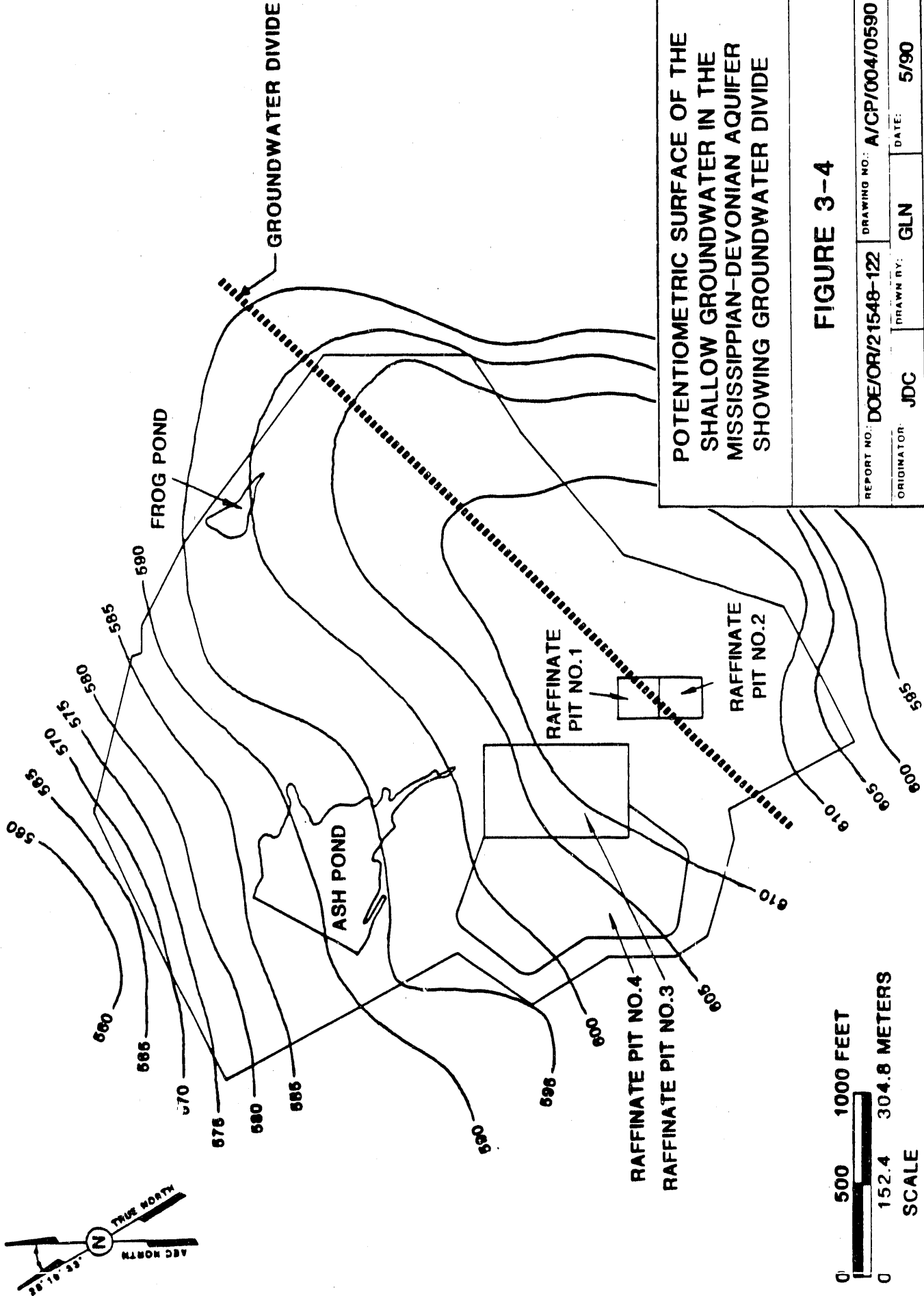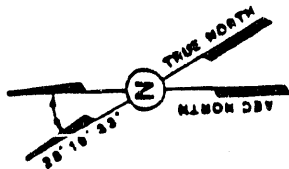
POTENTIOMETRIC SURFACE OF THE
SHALLOW GROUNDWATER IN THE
MISSISSIPPIAN-DEVONIAN AQUIFER
SHOWING GROUNDWATER DIVIDE

FIGURE 3-4
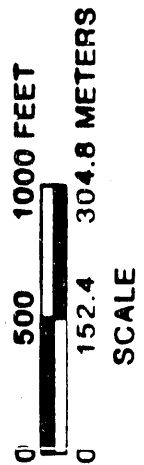
vertical fractures is approximately 20:1 or greater (MKF and JEG 1989b).

To provide insight into the degree of karst development and, consequently, the potential for conduit flow in the upper portion of the Mississippian-Devonian aquifer system, the following discussion of core recovery and drilling fluid loss is presented. Dissolution and weathering of the bedrock is indicated by poor core recovery in the upper 6 to 9 m (20 to 30 ft) of the bedrock in many locations; complete loss of circulation of drilling fluids during drilling of roughly half of the borings; dissolution features in cores; and low rock quality designation (RQD) values for the upper 3 to 15.25 m (10 to 50 ft) of bedrock cores (MKF and JEG 1990).

In general, core loss is concentrated in the top 6 to 9 m (20 to 30 ft) of bedrock with less than 1.5 m (5 ft) of core loss per boring. Notable exceptions include MW-4009 and MW-4010. MW-4009 experienced a total core loss of 7.6 m (24.9 ft) beginning at a depth of 17.1 m (56.2 ft) below ground surface and MW-4010 had 7.4 m (24.3 ft) of total core loss starting at a depth of 13.4-m (44 ft) below ground surface. These wells are located along the projection of the conduit traced from losing stream stretches that occur down-drainage from Ash Pond. A discussion of the effects of core loss and fluid loss during drilling is presented in the Report on Suitability of the Weldon Spring Site for Potential Location of a Disposal Facility (MKF and JEG 1990).

4 INVESTIGATION PROCEDURES

Three types of tests were performed to obtain the data included in this report: slug tests, pumping tests, and tracer tests. This section describes field procedures and the data management methods used for each type of test.

4.1 Slug Tests

Slug tests were performed on 39 monitoring wells, two geotechnical piezometers, and 28 observation wells between October 1988 and November 1989. The locations of wells and piezometers subjected to slug tests are presented in Figure 4-1. The testing was performed by Project Management Contractor (PMC) personnel in support of aquifer characterization efforts as detailed in the Hydrogeologic Investigations Sampling Plan (MKF and JEG 1988b). All of the wells selected for testing are screened within the Burlington-Keokuk Limestone which is the uppermost unit of the Mississippian-Devonian aquifer beneath the site. The results of these tests are expected to provide information on hydraulic conductivity and aquifer heterogeneity and anisotropy, and to complement pumping tests and water level and flow study data.

4.1.1 Field Procedures

Falling and rising head tests were conducted at each well using solid polyvinyl chloride (PVC) slugs attached to braided polypropylene rope. For 0.05 m (2 in.) inside diameter (ID) wells a 0.032 m (1.25 in.) diameter by 1.52 m (60 in.) long slug was used, and for 0.10 m (4 in.) ID wells a 0.076 m (3 in.) diameter by 1.52 m (60 in.) long slug was used. The 0.032 m

LOCATIONS OF MONITORING AND
OBSERVATION WELLS SUBJECTED
TO SLUG TESTS

FIGURE 4-1

REPORT NO.	DOE/OR/21548-122	EXHIBIT NO.	A/CP/096/1190
ORIGINATOR	JDC	DRAWN BY	GLN	DATE	11/90

▲ 1988 MONITORING WELL
○ PRE 1988 MONITORING WELL
⊘ OBSERVATION WELL ARRAY

SCALE

0   500   1000 FEET
0   152.4   304.8 METERS

(1.25 in.) diameter slug created a vertical head displacement of approximately 0.61 m (2 ft) and the 0.076 m (3 in.) diameter slug created a vertical displacement of approximately 1.52 m (5 ft). Head data were collected using an Enviro-Labs Model DL-120-MCP programmable data logger equipped with a 0-to-25-pound/sq in. (psi) pressure transducer.

Well numbers, depths to static water level, pressure transducer installation depths, initial transducer heads, test types (rising or falling), and test times were recorded in the field log book by field personnel. Variable interval sampling frequencies were also developed and recorded in the field.

In general, tests were conducted as follows:

1. The depth to static water level was determined and recorded.

2. The pressure transducer was placed in the well to a depth of approximately 2.5 m (8 ft) or more below the static water level.

3. A falling head test was performed by simultaneously starting data acquisition (using the data logger) and quickly lowering the PVC slug within the well to a depth below the previously determined static water level. Data acquisition proceeded until transducer head values closely approximated pretest conditions.

4. After transducer head values indicated a return to static or near static conditions, a rising head test was conducted by simultaneously starting data acquisition and withdrawing the PVC slug, thereby causing an instantaneous decrease in the transducer head value.

5. Data acquisition proceeded until head values returned to static or near static conditions whereupon testing was terminated.

4.1.2 Data Management

All data were collected using the EL-120-MCP data logger and pressure transducer. Field data were periodically transferred to a portable computer for conversion to a LOTUS 1,2,3 compatible format using an Environ-Labs data conversion program. Individual test identification for data analysis was accomplished using HYCON, a LOTUS program developed at the Weldon Spring Site Remedial Action Project (WSSRAP) specifically for single well hydraulic conductivity data reduction and analysis.

4.2 Pumping Tests

The pumping tests were designed to provide data to be used in the calculation of the transmissivity, storativity, and areal anisotropy of the shallow bedrock aquifer beneath the Weldon Spring chemical plant and raffinate pits (WSCP/RP). Pumping tests began January 10, 1989 and continued through February 4, 1989. These tests were performed by Earth Scientists, Inc. of St. Louis, Missouri, on behalf of the PMC, at pumping and observation well networks installed specifically for performance of pumping tests. The locations of pumping and observation well networks are indicated in Figure 4-2.

The following subsections describe the rationale used to design testing, the procedures followed in the performance of the pumping tests, and the methods used to manage the data obtained during the testing.

29

FROG POND

ASH POND

RAFFINATE PITS

OB1C OB1B OB1A PW1 OB1D OB1E OB1F
OB1I OB1G OB1H

OB2C OB2B OB2A PW2 OB2D OB2E OB2F
OB2J OB2G OB2H OB2I

OB3C OB3B OB3A PW3 OB3D OB3E OB3F
OB3I OB3G OB3H

MW-2012 MW-2013 MW-2006 MW-2010 MW-2011 MW-2018 MW-2016 MW-2007 MW-2005 MW-2001 MW-2002 MW-2003 MW-3003

■ PUMPING WELL
● OBSERVATION WELL
▲ MONITORING WELL

SCALE

0   1000   2000 FEET

0   304.8   609.6 METERS

N
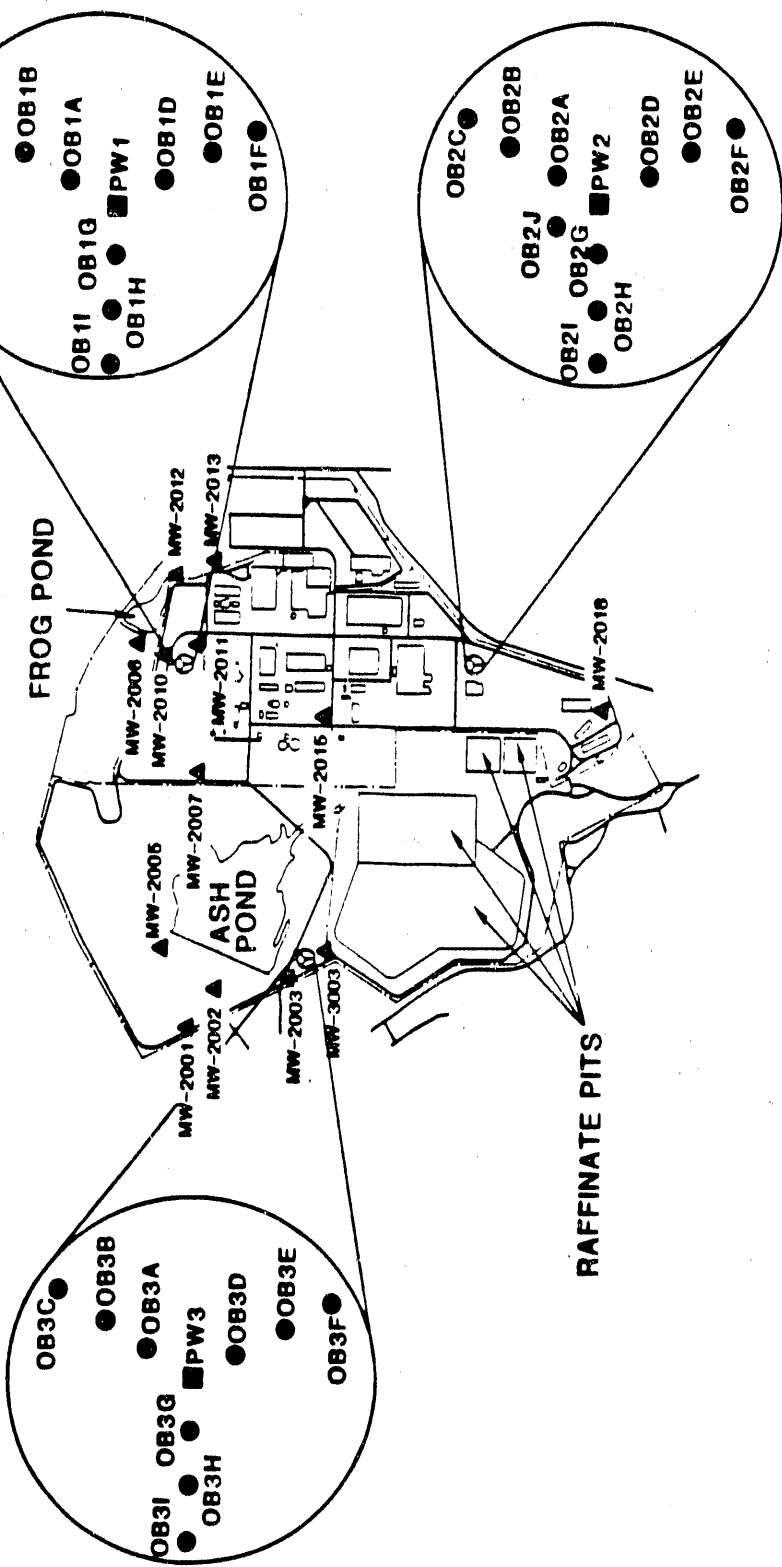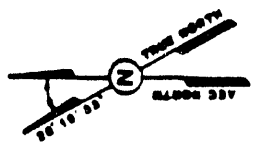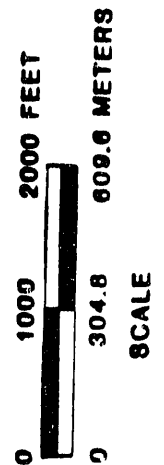
LOCATIONS OF WELLS USED
IN PUMPING TESTS

FIGURE 4-2

REPORT NO: DOE/OR/21548-122   DRAWING NO.: A/CP/005/0590

ORIGINATOR JDC   DRAWN BY: GLN   DATE: 5/90

4.2.1 Testing Rationale

As the pumping and observation wells were developed, step-drawdown pumping tests were performed. The results of these tests showed that it was likely that the pumping tests could be run concurrently to shorten the period of test performance. To monitor for possible interference between pumping wells, a staggered starting schedule was developed. According to the schedule, the initial pumping test would be run for a minimum of 48 hours. During that time, static water levels were observed so that any effects at other test locations could be identified. Assuming negligible effects at other locations, a concurrent pumping test could begin and the process could be repeated until completion of all testing.

Preliminary calculations indicated that up to 240 hours of pumping would be necessary at each pumping location to monitor potential effects of delayed yield under steady state conditions. However, contingency plans were made to end the pumping before this time limit if pumping could not be sustained. Maximum sustainable pumping rates were determined based on the results of step-drawdown pumping tests performed during well development.

4.2.2 Field Procedures

Before the first test was started, static water levels were observed to determine background conditions of the aquifer. Potentiometric observation began on January 10, 1989. Water level measurements were taken at two-hour intervals at the three pumping/observation well networks and selected monitoring wells near the pumping wells (Table 4-1). These measurements continued for approximately 96 hours.

During and after the testing, water levels were monitored at time intervals based on three schedules. These schedules are shown in Table 4-2.

Upon termination of pumping, recovery measurements were taken until the water level had returned to within 10% of the original static water level.

Water levels were monitored by two methods. The water levels in the pumping wells were monitored using pressure transducers. The information was recorded using data loggers manufactured by In Situ, Inc., Laramie, Wyoming. The electronic data were verified by obtaining water levels with an electric tape at periodic intervals. Electric tapes were also used to obtain all water levels in the observation and monitoring wells.

The pumping test at Well No. PW-2 began at 8:36 am, Friday, January 13, 1989 at a pumping rate of 1.5 lpm (0.4 gpm). Water level measurements continued at and around the other pumping locations. Pumping continued until 6:30 pm, Friday, January 20, 1989 -- a total of 178 hours. Pumping was terminated after the water level in the pumping well began dropping rapidly to near the level of the pump intake. Water level recovery was then monitored until 8:39 am, January 22, 1989, when the test was terminated.

The pumping test at Well No. PW-3 began at 1:42 pm, Wednesday, January 18, 1989 at a pumping rate of 1.1 lpm (0.3 gpm). Pumping continued until 10:25 am, January 26, 1989 -- a total of 189 hours. Pumping was terminated after the water level in the pumping well began dropping rapidly to near the level of the pump intake, approximately 36 hours after the well

TABLE 4-1   Water Level Monitoring Locations Used During
Pumping Tests

	Monitoring Locations	Well Depth (ft)	Screen Interval (ft)
PW-1	PW-1	90.3	49.5-89.5
	OB1A	89.5	48.0-89.0
	OB1B	91	50.5-90.5
	OB1C	88.5	48.0-88.0
	OB1D	90	49.5-89.5
	OB1E	94	54.0-94.0
	OB1F	93	52.5-92.5
	OB1G	90	49.5-89.5
	OB1H	93	53.0-93.0
	OB1I	90	49.5-89.5
	MW-2006	71	55.5-65.5
	MW-2007	99	83.0-93.0
	MW-2010	64	48.0-58.0
	MW-2011	79	62.8-72.8
	MW-2012	69.5	48.0-58.0
	MW-2013	75	58.0-68.0
PW-2	PW-2	89.8	45.0-85.0
	OB2A	85	44.5-84.5
	OB2B	85.5	45.0-85.0
	OB2C	85	44.5-84.5
	OB2D	85	44.5-84.5
	OB2E	86	45.5-85.5
	OB2F	84	43.5-83.5
	OB2G	85	44.5-84.5
	OB2H	85.5	45.0-85.0
	OB2I	86	45.5-85.5
	OB2J	143	130.0-140.0
	MW-2015	86	67.5-77.5
	MW-2018	69	53.0-63.0

TABLE 4-1   Water Level Monitoring Locations Used During
Pumping Tests (Continued)

Test Locations	Monitoring Locations	Well Depth (ft)	Screen Interval (ft)
PW-3	PW-3	86	45.5-85.5
	OB3A	83	42.5-82.5
	OB3B	85.1	44.6-84.6
	OB3C	83	42.5-82.5
	OB3D	83	42.5-82.5
	OB3E	85	45.0-84.5
	OB3F	83	42.5-82.5
	OB3G	83	42.5-82.5
	OB3H	85	45.0-84.5
	OB3I	83	42.5-82.5
	MW-2001	64	48.0-58.0
	MW-2002	64	48.0-58.0
	MW-2003	64	48.0-58.0
	MW-2005	81	65.5-75.5
	MW-3003	89.5	79.2-89.2

TABLE 4-2   Time Intervals for Measuring Drawdown During Pumping
Tests

Time Since Pumping Started/Stopped (Minutes)	Time Intervals Between Measurements
Pumping Tests	
0 - 1	1 sec.
1 - 5	10 sec.
5 - 10	30 sec.
10 - 15	1 min.
15 - 60	5 min.
60 - 240	30 min.
240 - 720	60 min. (1 hr.)
720 - 1440	120 min. (2 hr.)
1440 - termination of test	240 min. (4 hr.)
Observation Wells	
0 - 60	2 min.
60 - 120	5 min.
120 - 240	10 min.
240 - 360	30 min.
360 - 1440	60 min.
1440 - termination of test	480 min. (8 hr.)
Monitoring Wells	
0 - 12	1 min.
12 - 24	2 min.
24 - termination of test	4 min.

reached steady state. After pumping, water level recovery was monitored until 9:23 am, January 30, 1989.

The pumping test at PW-1 began at 12:55 pm, January 24, 1989 at a pumping rate of 1.1 lpm (0.3 gpm). Pumping continued for the planned 240-hour duration until 1:13 pm, February 3, 1989. Water level recovery was monitored until 1:08 pm, February 4, 1989.

4.2.3 Data Management

Field measurements from the pumping tests included static water levels, pumping and recovery water levels, ambient air temperature, and barometric pressure. Barometric pressure and temperature were recorded from a mercury barometer and a thermometer at the pumping well.

All physical measurements collected by the subcontractor were recorded in field notebooks and were then transferred to LOTUS 123 spreadsheets. Calculations were made to convert the field elevations to elevations above mean sea level and to correct for changes in atmospheric pressure. The final data were then transmitted to the PMC in hardcopy and electronic form.

4.3 TRACER TESTS

The tracer tests were designed to aid in determining values of effective porosity and assessing dispersivity. The tracer tests were performed at the PW-2 and PW-3 networks. PW-1 was not considered suitable for tracer tests due to its susceptibility to freezing and proximity to known areas of nitroaromatic compound contamination. Figure 4-3 shows the location of the injection points at each test network. The following subsections describe

POTASSIUM BROMIDE TRACER INJECTION POINT

FROG POND

POTASSIUM CHLORIDE TRACER INJECTION POINT

POTASSIUM BROMIDE TRACER INJECTION POINT

POTASSIUM CHLORIDE TRACER INJECTION POINT

MW-2012
MW-2013
MW-2008
MW-2010
MW-2011
MW-2018
MW-2015
MW-2007
MW-2006
ASH POND
MW-2001
MW-2002
MW-2003
MW-3003

RAFFINATE PITS

PUMPING WELL
OBSERVATION WELL
MONITORING WELL

| 0 | 1000 | 2000 FEET |
| 0 | 304.8 | 609.6 METERS |

SCALE
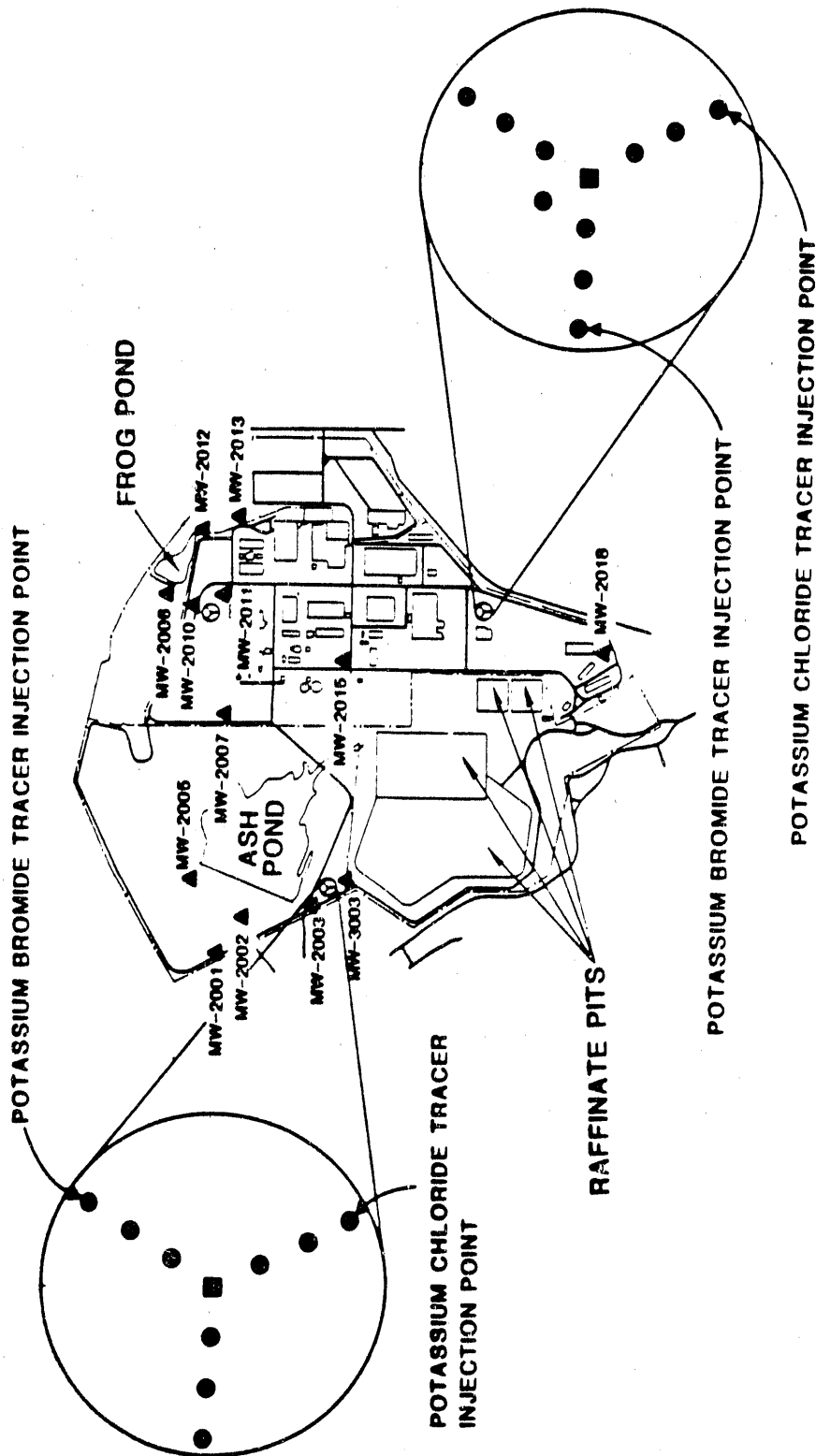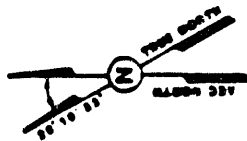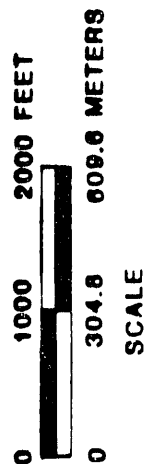
LOCATIONS OF OBSERVATION WELLS
USED AS TRACER INJECTION POINTS

FIGURE 4-3

REPORT NO.: DOE/OR/21548-122 DRAWING NO.: A/CP/008/0590

ORIGINATOR JDC DRAWN BY: GLN DATE: 5/90

the procedures followed in the performance of the tests and the methods used to manage the data as it was collected.

4.3.1 Field Procedures

A converging-flow technique was selected in which an aliquot of conservative ion tracer solution was injected into observation wells and samples were collected from the pump discharge at preset intervals. Chloride and bromide salts were selected as tracers because they are environmentally safe, readily available, and could be easily analyzed on site at parts-per-million levels using a specific ion electrode. Tracers were prepared by dissolving 5 kg (11 lb) of potassium bromide or potassium chloride in 8-liters (2.1 gallons) of deionized water. Two tracer tests were conducted at each location using different ion solutions to determine effects of anisotropy on travel time. Preliminary estimates indicated that 100 to 150 hours would be required for the tracers to travel from the injection well to the pumping well under the anticipated pumping rates.

Samples were collected in 250 ml Nalgene bottles according to the schedule shown in Table 4-3. New bottles were obtained specifically for the tracer testing but were reused as necessary. Prior to each use, the bottles were triple-rinsed with deionized water and immediately before a sample was taken were triple-rinsed with water from the pump discharge. At each sampling time, a total of four samples was taken from each well. This gave duplicate samples for each tracer analysis.

Pumping for the tracer tests at PW-3 began at 3:45 pm, March 21, 1989. A saturated potassium chloride solution was injected into observation well OB3C on March 22 between 3:15 pm and

TABLE 4-3 Sampling Intervals During Tracer Testing

Time Since Tracer Injection (hours)	Time Interval Between Samples (hours)
0 - 24	No Samples Taken
24 - 96	4
96 - termination of test	2

4:20 pm. A saturated potassium bromide solution was injected into observation well OB3F between 4:40 pm and 4:55 pm. After the tracers were injected at each location, each injection well was surged with a bailer to mix the tracer within the water column. Then a total of 275 liters (73 gallons) of aquifer water from the pump discharge was injected incrementally as a "chaser" to drive the tracer into the formation. Sample collection at the pumping well began at 4:00 pm, March 22 and continued until the test was terminated at 4:40 pm, April 12.

Pumping for the tracer tests at PW-2 began at 4:40 pm, March 22, 1989. A saturated potassium chloride solution was injected into observation well OB2I on March 24 between 9:30 am and 9:50 am, and a saturated potassium bromide solution was injected into observation well OB2E between 2:30 pm and 2:42 pm. Surging and injection of chaser water followed the tracer injections in the same manner as at the PW-3 location. Sample collection at the pumping well began at 12:30 am, March 25 and continued until the test was terminated at 4:50 pm, April 12.

4.3.2 Data Management

The measurements taken during the tracer tests were the same as those taken during the pumping tests with the addition of tracer concentrations. The tracer concentrations were determined by analyzing the water samples taken from the pumping wells using specific-ion electrodes attached to an Orion meter. Meter calibration curves were generated using standards of 1 part per million (ppm), 10 ppm, and 100 ppm for bromide and 10 ppm, 100 ppm, and 1,000 ppm for chloride. The calibration curves and slope intercept equation were used to convert millivolt readings to parts per million.

5 METHODS OF ANALYSIS

Monitoring wells, pumping wells, and observation wells were utilized for aquifer testing at the Weldon Spring chemical plant/ raffinate pits/vicinity properties (WSCP/RP/VP) in support of the environmental documentation process. The primary objectives of testing were to define the hydraulic characteristics of the aquifer. This information will be of use in predicting contaminant migration and in assessing groundwater remediation alternatives. Slug tests were performed to provide information on areal variations in hydraulic conductivity in the uppermost aquifer. Pumping tests were performed to accurately determine transmissivity and specific yield and to allow assessment of the effects of pumping on groundwater flow patterns and contaminant levels. Tracer tests were performed to assess the effective porosity and dispersive properties of the formation. The methods of analysis used to evaluate the slug tests, pumping tests, and tracer tests are discussed in this section.

5.1 SLUG TESTS

Test data were analyzed using two analytical methods. A method developed by Hvorslev (1951) was used to determine hydraulic conductivity. This method allowed comparisons because it is widely used. A method developed by Bouwer and Rice (1976) was also used to derive hydraulic conductivity values.

Slug test head recovery data revealed three types of data configurations that required examination and editing prior to analysis. These data configurations were:

Harmonic distortion - This occurs when a pressure wave is created during slug deployment. Since the transducer used to collect

data converts pressure to hydrostatic head in units of length, the force of slug deployment results in variations in pressure (head) at the transducer. These variations may be either greater than or less than actual head differences due to differences in aquifer hydraulic conductivity. The pressure wave created during slug deployment was generally observed to dissipate within the first 5 to 10 seconds of the test. Harmonic distortion was easily recognized during data inspection because head values within the distorted data segment usually exceeded the possible range of head values caused by slug deployment. Data segments exhibiting harmonic distortion were not included during data analysis. The omission of early time data did not impact the quality of data analysis since early time data segments reflected filterpack influences in most cases.

Level shifts - Data sets that exhibited instantaneous (vertical) shifts in head level that were not consistent with the established recovery rate were examined. It was found that the vertical shifts always occurred at programmed changes in collection frequency. Level shifts were not common. Retesting usually yielded acceptable data; however, in a few cases, the data were smoothed manually to reflect the pre-shift and post-shift recovery rates.

Filterpack influence - Most tests exhibited a dramatic decrease in the rate of head recovery within the first 5 to 30 seconds of data recovery. The fast early time recovery rate is attributed to the permeability of the filterpack material surrounding the screen. These portions of the data are easily recognized upon inspection and were not utilized for data analysis.

5.1.1 Hvorslev Method

The Hvorslev method is the simplest interpretation of piezometer recovery data under unconfined conditions. The analysis assumes a homogeneous, isotropic medium of infinite vertical extent, where the medium and fluid are incompressible and the change in volume of fluid within the borehole is instantaneous.

In the Hvorslev method, linear regression is used on a plot of the log of the ratio of the difference in head at any time during the test to the head difference at the beginning of the test (ln [H-h/H-H0]) versus time to determine the basic time lag, T_o. Hvorslev defines T_o as the time required for equalization of the active head while maintaining the original rate of flow. Hydraulic conductivity is then expressed as follows:

$$K = \frac{r^2 \ln (L/R)}{2LT_o}$$

(1)

where:

r   = radius of the casing
L   = length of the intake
R   = radius of the borehole at the intake
T_o = basic time lag

The basic geometry and graphical determination of T_o for the Hvorslev method are presented in Figure 5-1.

a) GEOMETRY

b) GRAPHICAL ANALYSIS

(SOURCE: FREEZE AND CHERRY, 1979)
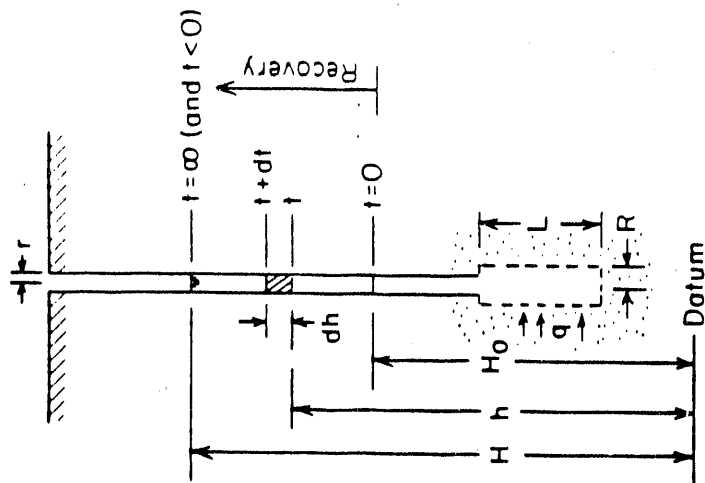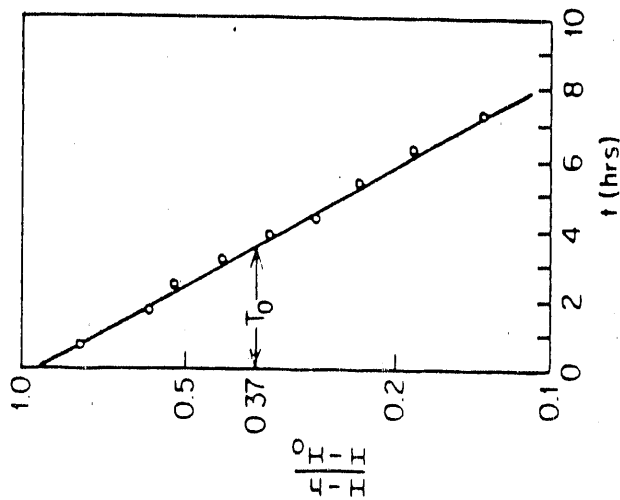
SLUG TEST GEOMETRY:
HVORSLEV METHOD

FIGURE 5-1

REPORT NO: DOE/OR/21548-122	DRAWING NO.: A/PI/011/0590	
ORIGINATOR: JDC	DRAWN BY: GLN	DATE: 5/90

5.1.2 Bouwer and Rice Method

The method developed by Bouwer and Rice is derived from a modification of the Thiem equation where:

$$Q = \frac{2\pi K L y}{\ln(R_e/r_w)}$$

(2)

and the hydraulic conductivity is determined for an unconfined system by:

$$K = \frac{r_c^2 \ln(R_e/r_w) \ln(y_o/y_t)}{2Lt}$$

(3)

where:

K = hydraulic conductivity

r_c = radius of well casing

r_w = radius of borehole at the intake

L = length of intake

t = time

R_e = effective radius over which y is dissipated

y = the vertical distance between the water in the well at time zero (y_o) or any time during the test (y_t) and the potentiometric surface at equilibrium

Test geometry for the Bouwer and Rice analysis is illustrated in Figure 5-2.

The change in head, y, was plotted versus time, t, (see Figure 5-2) to determine the appropriate straight line portion of the data for analysis. Most of the data exhibited a double straight line effect wherein data within the first 5 to 7 seconds exhibited a sharp decline in head difference, followed by a flattening of the time-versus-head relationship. In all cases the second straight line portion of the data was considered to reflect aquifer response. The terms $1/t$ and y_o/y_t were determined graphically as suggested by Bouwer (1989). Data plots are contained in controlled files maintained at the WSS project office. The data files are available for review on request. The straight line data portions used for analysis typically encompass later time data (up to 780 seconds) than that addressed by Bouwer (1989) in his update. However, it should be kept in mind that head-recovery curves for low permeability aquifers seldom resemble the example data plots used to illustrate principles of hydraulic phenomena.

Head recovery data were considered to reflect conditions closely approximating a fully penetrating situation where D is effectively equal to the distance between the potentiometric surface and the bottom of the test interval (screen). Fully penetrating conditions were assumed due to a conceptual model of anisotropy within the Burlington-Keokuk where hydraulic conductivity in the horizontal planes (K_x and K_y) are considered to be much greater than hydraulic conductivity in the vertical plane (K_z).

2008_R01

b)

DELTA t (sec)

DELTA y (ft)

a) GEOMETRY
b) EXAMPLE DATA PLOT

SOURCE: FIGURE 5-2a FROM BOUWER, 1989
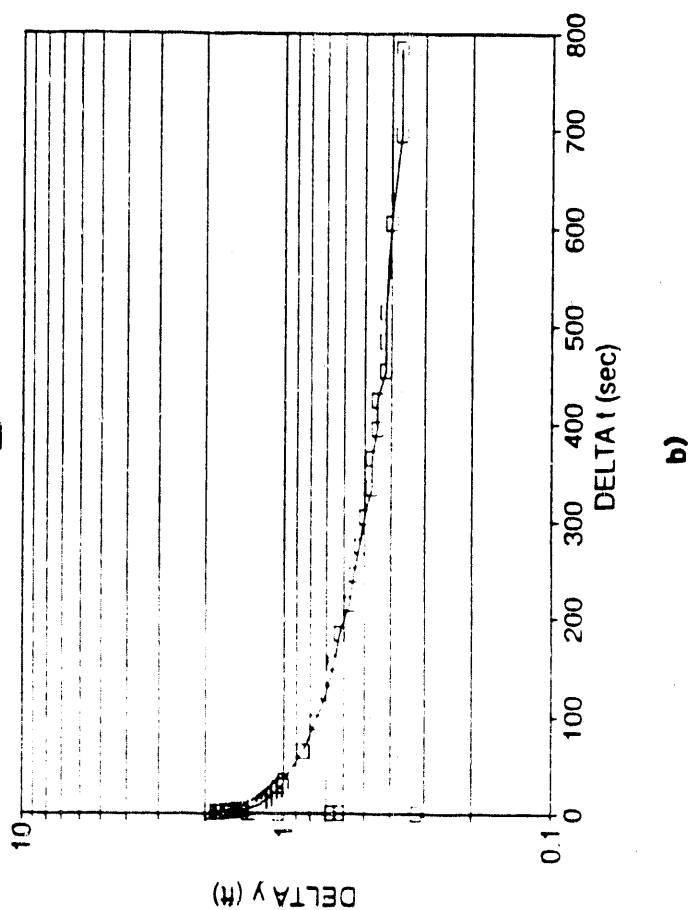
5.2 PUMPING TESTS

Pumping tests were designed to assess the reasonableness of the assumption that the shallow Mississippian-Devonian aquifer beneath the site can be modeled as an equivalent homogeneous porous medium exhibiting areal anisotropy in the horizontal plane.

Data obtained from the pumping tests were used to determine three properties of the upper portion of the Mississippian-Devonian aquifer beneath the WSCP/RP/VP: transmissivity, storativity, and lateral anisotropy. Values of transmissivity and storativity were obtained using the Cooper-Jacob (time-drawdown) semi-log method (Cooper and Jacob 1946). Anisotropy was determined using the Hantush method, which also yields values for transmissivity and storativity. Secondary objectives were to review the available data for evidence of other significant hydrologic phenomena, such as delayed yield due to gravity drainage, boundary effects, and leakage effects, which might provide insight into the presence and relative magnitude of double porosity as may be expected in an aquifer consisting of limited intergranular and fine fracture porosity coupled with larger aperture fractures and solution features.

In order to perform the Cooper-Jacob method, the data were plotted semi-logarithmically with drawdown on the y-axis and time plotted logarithmically on the x-axis. A line was then plotted through the straight line portion of the data and extended to find the intercept of the line of zero drawdown. Figure 5-3 is an example of the graphical determination of zero drawdown. The following equations were then applied.

DRAWDOWN CURVE

Δs

t_o

Δt (LOGARITHMIC SCALE)
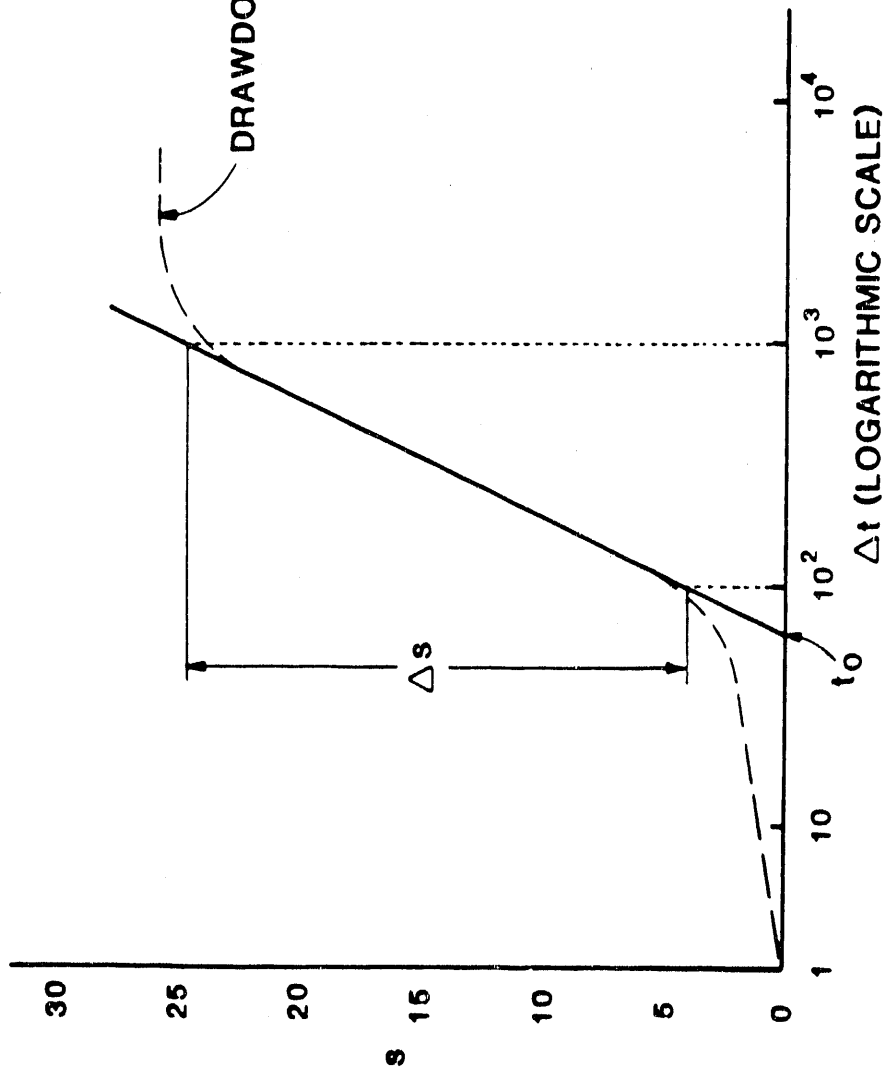
EXAMPLE OF COOPER–JACOB GRAPHICAL
METHOD OF PUMPING TEST ANALYSIS

FIGURE 5-3

| REPORT NO | DOE/OR/21548–122 | DRAWING NO : | A/PI/013/0590 |
| ORIGINATOR | JDC | DRAWN BY GLN | DATE 5/90 |

$$T = 264Q/s \qquad (4)$$

$$S = Tt_o/4800r^2 \qquad (5)$$

where:

T = transmissivity (gpd/ft)

Q = pumping rate (gpm)

s = change in drawdown per log cycle (ft/cycle)

S = storativity (dimensionless)

t_o = x-intercept of straight line portion of curve (minutes)

r = distance from pumping well to observation well (ft)

The resulting values of T and S are average values for the formation in the area between the pumping well and the specific observation well. The values also overlap along the lines of the observation wells.

The Hantush method provides a measure of the lateral anisotropy of a formation. Intermediate steps in the method also provide storativity and minimum and maximum transmissivity values. A summary of the analysis follows (Hantush and Thomas 1966).

Values of transmissivity and storativity are obtained for each observation well using a standard technique, such as the Cooper-Jacob method. These values of transmissivity are then averaged to obtain an effective transmissivity, T_e, of the system. The drawdown values, s, at a given time, t_t, are then plotted, and for a given drawdown, an ellipse is contoured with major and minor axes, A and B, respectively. The orientation of the ellipse, $\emptyset$, can be found graphically (Figure 5-4). The principal values of the transmissivity in the major and minor

MAJOR AXIS

MINOR AXIS

EQUIVALENT
DRAWDOWN
ISOPLETH
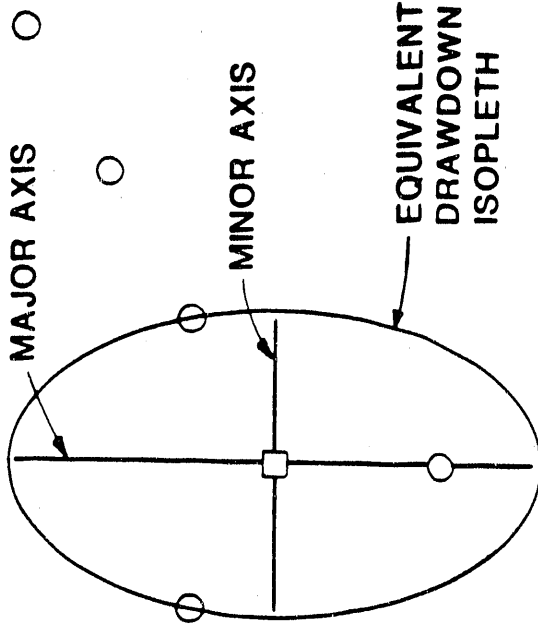
○ OBSERVATION WELL

□ PUMPING WELL

1. PLOT SYNCHRONOUS DRAWDOWN AT EACH OBSERVATION WELL

2. DRAW ISOPLETH FOR EQUAL DRAWDOWNS

3. DETERMINE DIRECTION OF MAJOR AND
MINOR AXES OF RESULTING ELLIPSE

EXAMPLE OF HANTUSH METHOD
FOR DETERMINING DEGREE AND
DIRECTION OF ANISOTROPY

FIGURE 5-4

REPORT NO: DOE/OR/21548-122	DRAWING NO: A/PI/014/0590
ORIGINATOR: JDC	DRAWN BY: GLN	DATE: 5/90

directions of the ellipse and the principal anisotropy can then be found from the following set of equations:

$$T_{max} = (a/b)T_e \tag{6}$$
$$T_{min} = (b/a)T_e \tag{7}$$
$$S = (4T_e t_f/ab)W^{-1}(4T_e s/Q) \tag{8}$$
$$\text{Principal Anisotropy} = T_{max}/T_{min} \tag{9}$$

where:

T_{max} = maximum transmissivity

T_{min} = minimum transmissivity

W^{-1} = inverse well function

Q = pumping rate

5.3 TRACER TESTS

Data obtained from the tracer tests were used to assess the effective porosity and dispersivity of the formation. Determination of the effective porosity was made using Darcy's law and the dispersivity was found by first using a common transport equation to find the hydrodynamic dispersion and then solving a direct relationship between hydrodynamic dispersion and dispersivity.

Darcy's law states that the specific discharge per unit area, q, of a formation is the product of the hydraulic conductivity, K, of the formation and the hydraulic gradient, i, across the formation. In order to obtain the effective porosity, n, the relationship q = vn, where v is the average linear velocity of the groundwater, must be substituted into Darcy's equation.

The hydraulic conductivity of the formation along the path of the tracer was found by dividing the transmissivity by the saturated thickness. In this case, the saturated thickness was taken to be the screened interval of the wells (40 feet). Equating saturated thickness to the screened interval ·is justified by the relative lack of vertical flow observed in the system (BNI 1987 and MKF and JEG 1989b). The transmissivity values that were used were estimated from the ellipses obtained in the Hantush analysis. The average hydraulic gradient between the injection well and pumping well, which is the value used in the calculation of effective porosity, is found by dividing the difference in hydraulic head between the injection and pumping wells by the distance between the two wells. Chloride and bromide ions are very conservative tracers, and therefore can be assumed to travel at the same velocity as the groundwater. Consequently, the average linear velocity can be determined by examining the breakthrough times of the tracers (Figure 5-5).

In order to find the dispersivity of the formation, the hydrodynamic dispersion, D_x, must first be determined. Hydrodynamic dispersion is found using the following transport equation (Bear 1972):

$$CA = \frac{M/n}{(4\pi D_x t)^{1/2}} \exp \left(\frac{(-x-Vt/n)^2}{4D_x t} \right)$$

(10)

where: C = tracer concentration in sample
        A = cross sectional area which the tracer originally occupies
        M = original tracer mass
        n = effective porosity of the formation
        D_x = hydrodynamic dispersion

CONCENTRATION
OF TRACER AT
PUMPED WELL

PEAK CONCENTRATION
CORRESPONDING TO
CENTROID OF TRACER PLUME

REDUCTION OF TRACER
CONCENTRATION AS SLUG
PASSES

BEGINNING OF
TRACER
BREAKTHROUGH

t_c

time

t_c = ARRIVAL TIME OF CENTROID

t   = time at which concentration, C, is determined

x   = distance that tracer travels

v   = average linear velocity of the groundwater

This equation is then rearranged to the form:

$$\frac{1}{D_x} \ln \frac{(M/n)}{(4\pi D_x t)^{1/2}} = - \frac{4t \ln(CA)}{(x - vt/n)^2}$$

(11)

and D_x is found through iterative solutions of the equation.

Dispersivity is related to the hydrodynamic dispersion by the equation:

$$D_x = V\alpha_x + D^*$$

(12)

where:

α_x = dispersivity

D^* = coefficient of molecular diffusion

Because the coefficient of molecular diffusion is several orders of magnitude smaller than the other terms, on the order of 10^{-10} (Freeze and Cherry 1979), it can be considered negligible and therefore can be omitted from the equation. Then, rearranging the resulting equation, dispersivity equals the coefficient of molecular diffusion divided by the average linear velocity.

6 RESULTS AND DISCUSSION

In the following sections the results of the slug tests, pumping tests, and tracer tests are presented and discussed.

6.1 Slug Tests

Statistical analyses of slug test results were performed to facilitate presentation of results. Figure 6-1 shows the distribution of results of slug test data analyzed by the Bouwer and Rice method for all monitoring wells and piezometers tested. Values for each observation well network are average values of all observation wells tested at each network location. A frequency histogram and summary statistics for all wells tested are presented in Figure 6-2. Individual slug test data for all wells tested are contained in controlled files maintained at the project office.

6.1.1 Monitoring Wells and Piezometers

Table 6-1 presents hydraulic conductivity values obtained by the Hvorslev and Bouwer and Rice methods for all monitoring wells and piezometers tested. Monitoring well designations are denoted by a MW prefix followed by a four-digit number, and piezometers are denoted by a GT prefix followed by a two-digit number and a P suffix.

Analysis by the Hvorslev method yielded results which ranged from a high of 1.4 m/d (5.3E-05 ft/s) for MW-4014 to a low of 1.4E-03 m/d (5.35E-08 ft/s) for MW-4011. A frequency histogram and summary statistics are provided in Figure 6-3.

TO CONVERT FROM METERS/DAY (m/d) TO
FEET/DAY (ft/d) MULTIPLY BY 3.28

DISTRIBUTION OF SLUG TEST RESULT.

BOUWER AND RICE METOD
(METERS/DAY)

FIGURE 6-1

REPORT NO. DOE/OR/21548-122	DRAWING NO.: A/CP/007/0590		
ORIGINATOR: JDC	DRAWN BY: GLN	DATE: 5/90

▲ 1988 MONITORING WELL
○ PRE 1988 MONITORING WELL
⊘ OBSERVATION WELL ARRAY

SCALE

BOUWER AND RICE METHOD

FREQUENCY (ALL WELLS)

HVORSLEV METHOD

FREQUENCY (ALL WELLS)
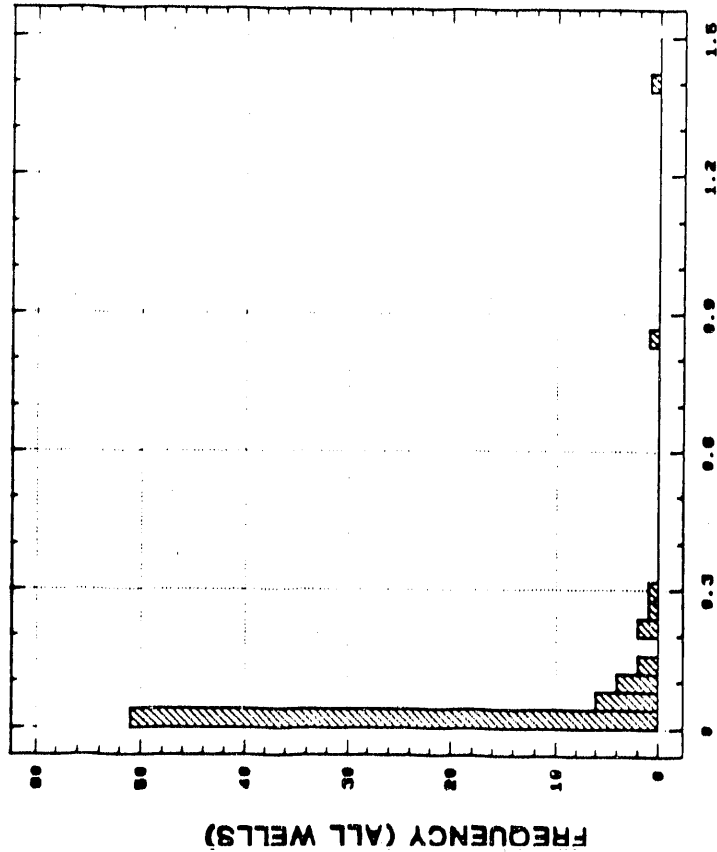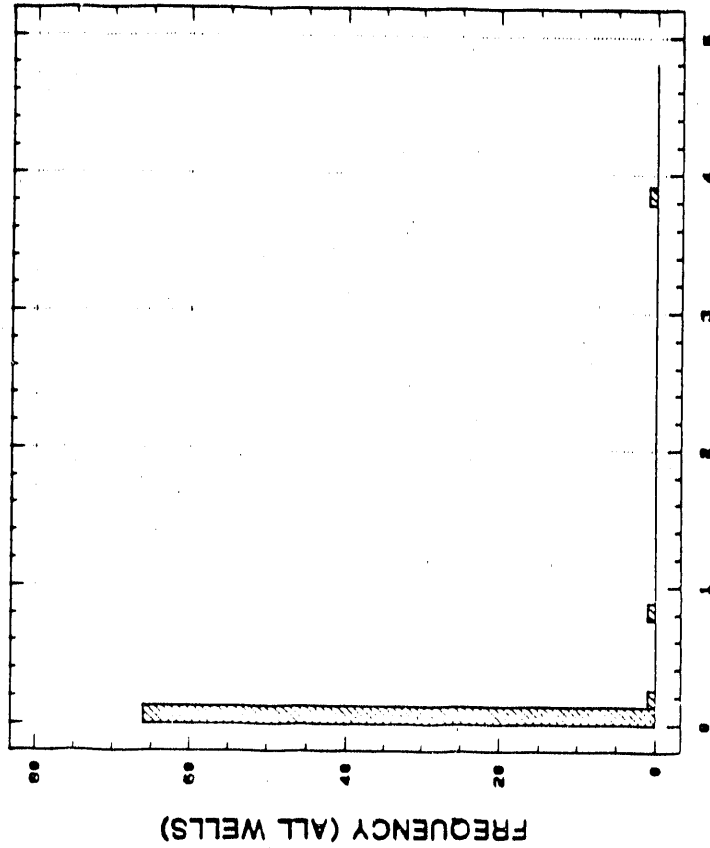
Variable:	HVORSLEV	BOUWER & RICE
Sample size	69	69
Average	0.0736072	0.0955145
Median	0.025	0.02
Standard deviation	0.196497	0.476955
Minimum	1.4E-3	1.5E-3
Maximum	1.4	3.9
Range	1.3986	3.8985

TO CONVERT FROM METERS/DAY (m/d) TO FEET/DAY (ft/d) MULTIPLY BY 3.28.

FREQUENCY HISTOGRAM AND SUMMARY STATISTICS OF SLUG TEST RESULTS FOR ALL WELLS TESTED (METERS/DAY)

FIGURE 6-2

TABLE 6-1   Slug Test Values for Monitoring Wells and Piezometers

WELL ID	MID-SCREEN DEPTH BELOW TOP BDRK (m)	MEAN HYDRAULIC CONDUCTIVITY (m/d)* Hvorslev Method	Bouwer & Rice Method	RATIO OF HVORSLEV/ BOUWER &
MW-2002	8.74	1.20E-01	6.50E-02	1.85
MW-2005	7.88	2.20E-02	1.80E-02	1.22
MW-2006	11.56	1.20E-01	5.90E-02	2.03
MW-2008	5.64	1.10E-01	5.10E-02	2.16
MW-2013	10.83	9.50E-02	4.10E-02	2.32
MW-2015	9.76	4.20E-02	1.00E-01	0.42
MW-2018	7.78	2.10E-01	5.70E-02	3.68
MW-2019	24.14	7.00E-03	1.70E-02	0.41
MW-2021	24.86	2.00E-02	2.10E-02	0.95
MW-2022	23.24	2.50E-02	3.50E-02	0.71
MW-2023	9.64	6.60E-03	7.90E-03	0.84
MW-2024	28.24	3.30E-02	3.40E-02	0.97
MW-2025	20.77	3.30E-02	3.40E-02	0.97
MW-2026	28.41	1.50E-02	2.90E-02	0.52
MW-2027	26.50	1.00E-02	1.20E-02	0.83
MW-2028	24.49	1.50E-02	1.50E-02	1.00
MW-2029	19.32	1.50E-03	1.50E-03	1.00
MW-3003	18.15	5.30E-03	5.00E-03	1.06
MW-3006	30.65	2.60E-01	2.30E-01	1.13
MW-3019	13.51	6.00E-02	4.70E-02	1.28
MW-4001	6.41	5.30E-02	4.30E-02	1.23
MW-4004	14.18	3.30E-03	5.50E-03	0.60
MW-4005	13.24	2.80E-03	3.60E-03	0.78
MW-4007	20.13	6.00E-03	6.60E-03	0.91
MW-4008	16.36	8.50E-03	8.90E-03	0.96
MW-4009	16.04	5.60E-03	5.80E-03	0.97
MW-4010	17.14	2.50E-03	4.30E-03	0.58
MW-4011	12.29	1.40E-03	1.50E-03	0.93
MW-4012	11.38	2.30E-03	3.90E-03	0.59
MW-4013	4.39	8.30E-01	4.90E-02	16.94
MW-4014	6.07	1.40E+00	8.80E-01	1.59
MW-4015	12.22	7.00E-03	2.50E-02	0.28
MW-4016	14.85	2.20E-02	3.50E-02	0.63
MW-4017	12.05	3.60E-02	2.60E-02	1.38
MW-4018	9.01	3.30E-02	2.60E-02	1.27
MW-4020	7.87	2.50E-02	2.00E-02	1.25
MW-4021	10.52	5.20E-02	3.40E-02	1.53
MW-4022	13.36	7.90E-02	2.00E-02	3.95
MW-4023	4.58	3.60E-03	6.70E-02	0.05
GT58P	7.47	2.00E-01	3.90E+00	0.05
GT66P	5.58	3.00E-01	5.50E-02	5.45

* To convert from meters/day (m/d) to feet/day multiply by 3.28

RICE

BOUWER AND RICE METHOD

FREQUENCY (MW'S & PIEZOMETERS)

HVORSLEV METHOD

FREQUENCY (MW'S & PIEZOMETERS)
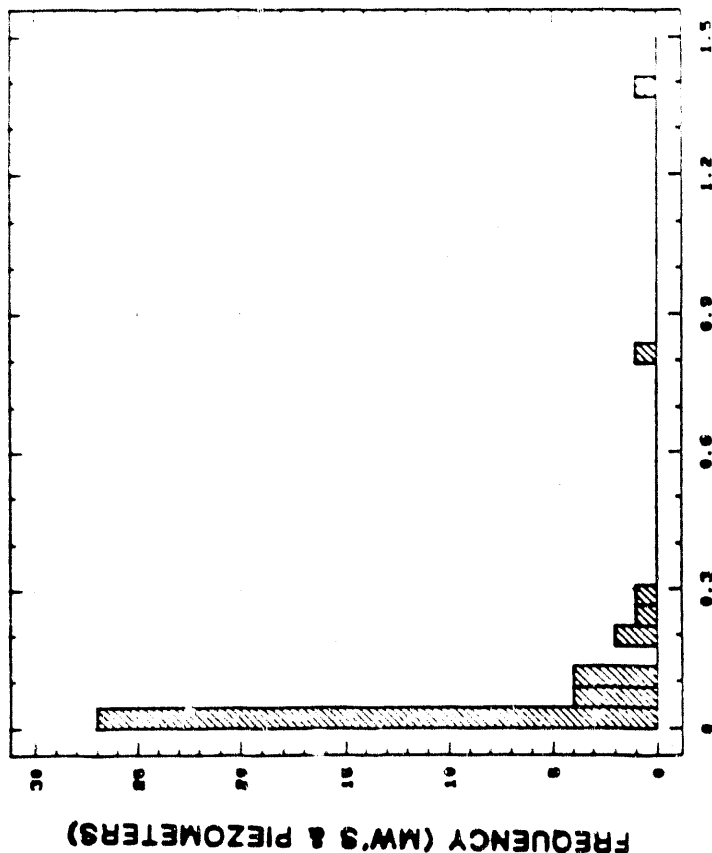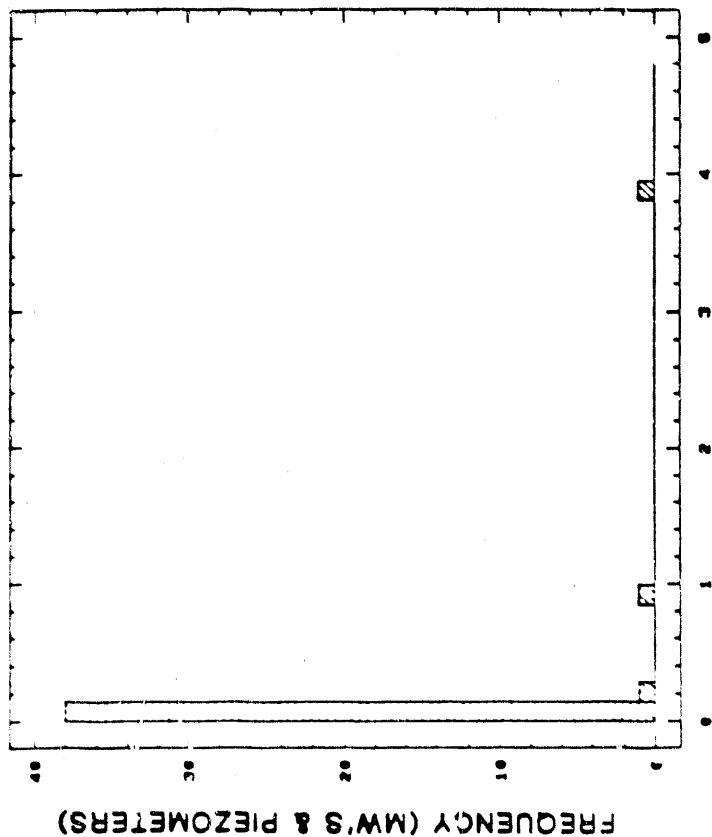
Variable:	HVORSLEV	BOUWER & RICE
Sample size	41	41
Average	0.104473	0.148768
Median	0.025	0.026
Standard deviation	0.25091	0.616043
Minimum	1.4E-3	1.5E-3
Maximum	1.4	3.9
Range	1.3986	3.8985

TO CONVERT FROM METERS/DAY (m/d) TO
FEET/DAY (ft/d) MULTIPLY BY 3.28

FREQUENCY HISTOGRAM AND SUMMARY
STATISTICS OF SLUG TEST RESULTS
FOR MONITORING WELLS AND
PIEZOMETERS (METERS/DAY)

FIGURE 6-3

Analysis by the Bouwer and Rice method yielded results which
ranged from a high of 3.9 m/d (1.5E-04 ft/s) for GT-58P to a low
of 1.5E-03 m/d (5.7E-08 ft/s) for MW-2029 and MW-4011. Summary
statistics and a frequency histogram are presented in Figure 6-3.
Data from piezometer GT58P was not suitable for analysis using
the Hvorslev technique due to almost instantaneous equalization
of that portion of the active head required for determination of
the basic time lag. Use of a potable water slug to create a
larger head displacement would probably eliminate this effect.

6.1.2 Observation Wells

Table 6-2 presents values obtained by Hvorslev and Bouwer and
Rice methods for all observation wells tested. As with the
monitoring well and piezometer data, values are either a mean or
single test value depending on the integrity of the test data.
Analysis by the Hvorslev method yielded results ranging from a
maximum of 1.0E-01 m/d (3.8E-06 ft/s) for OB2I to a minimum of
8.1E-03 m/d (3.1E-07 ft/s) for OB2J.

Analysis by the Bouwer and Rice method yielded results
ranging from a maximum of 4.4E-02 m/d (1.7E-06 ft/s) for OB3I and
a minimum of 6.5E-03 m/d (2.5E-07 ft/s) for OB2J. Frequency
histograms and summary statistics are presented in Figure 6-4.

6.1.3 Discussion

Calculated hydraulic conductivity values were compared by
dividing the value obtained using the Hvorslev Method with the
value obtained using the Bouwer and Rice Method. Ratios of
Hvorslev to Bouwer and Rice values average 1.6 and range from
0.05 to 16.94. Individual ratios are included in Table 6-1.

7

1

0790

TABLE 6-2 Slug Test Values for Observation Wells

WELL ID	MID-SCREEN DEPTH BELOW TOP BDRK (m)	MEAN HYDRAULIC CONDUCTIVITY (m/d)* Hvorslev Method	Bouwer & Rice Method	RATIO OF HVORSLEV/ BOUWER &
OB1A	3.58	1.80E-02	1.30E-02	1.38
OB1B	3.93	1.30E-02	1.10E-02	1.18
OB1C	3.55	1.00E-02	8.20E-03	1.22
OB1D	3.57	1.60E-02	1.70E-02	0.94
OB1E	3.86	1.60E-02	1.10E-02	1.45
OB1F	3.46	2.80E-02	2.30E-02	1.22
OB1G	3.60	9.80E-03	6.80E-03	1.44
OB1H	3.80	2.50E-02	1.70E-02	1.47
OB1I	3.56	1.70E-02	1.90E-02	0.89
OB2A	1.93	1.10E-02	7.50E-03	1.47
OB2B	2.19	3.60E-02	1.50E-02	2.40
OB2C	1.88	3.90E-02	2.10E-02	1.86
OB2D	1.99	3.70E-02	1.60E-02	2.31
OB2E	2.11	6.20E-02	3.60E-02	1.72
OB2F	2.03	3.90E-02	2.70E-02	1.44
OB2G	2.04	3.70E-02	2.00E-02	1.85
OB2H	2.17	2.40E-02	1.50E-02	1.60
OB2I	1.99	1.00E-01	3.40E-02	2.94
OB2J	8.72	8.10E-03	6.50E-03	1.25
OB3A	2.53	1.90E-02	1.00E-02	1.90
OB3B	2.92	1.70E-02	1.10E-02	1.55
OB3C	0.03	1.90E-02	1.30E-02	1.46
OB3D	2.48	2.80E-02	1.80E-02	1.56
OB3E	2.82	2.70E-02	1.70E-02	1.59
OB3F	2.49	8.60E-03	1.30E-02	0.66
OB3G	2.50	3.50E-02	2.10E-02	1.67
OB3H	2.67	3.00E-02	2.00E-02	1.50
OB3I	2.53	6.60E-02	4.40E-02	1.50

* To convert meters/day (m/d) to feet/day multiply by 3.28.

RICE

BOUWER AND RICE METHOD

HVORSLEV METHOD

FREQUENCY (OB'S)
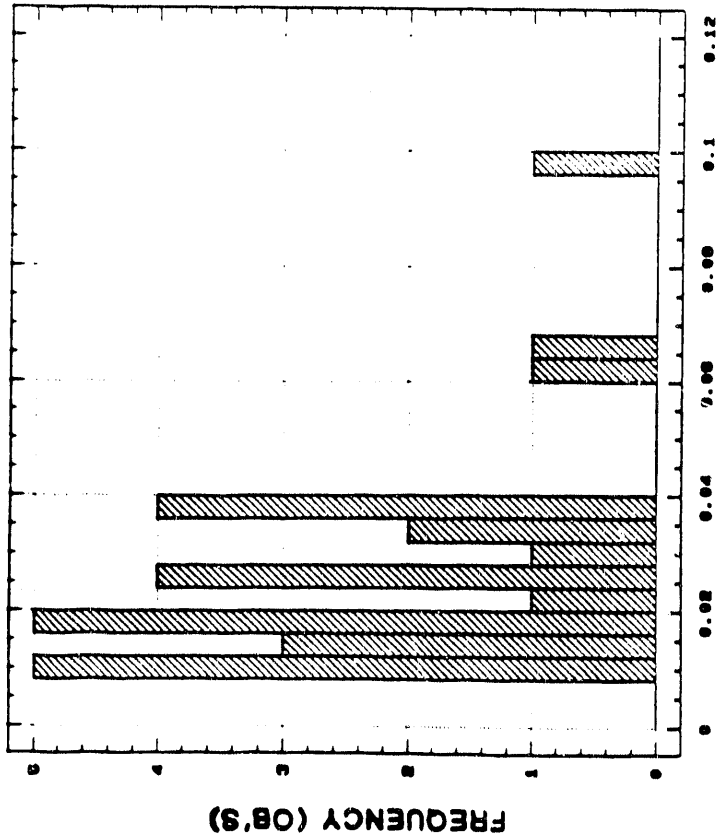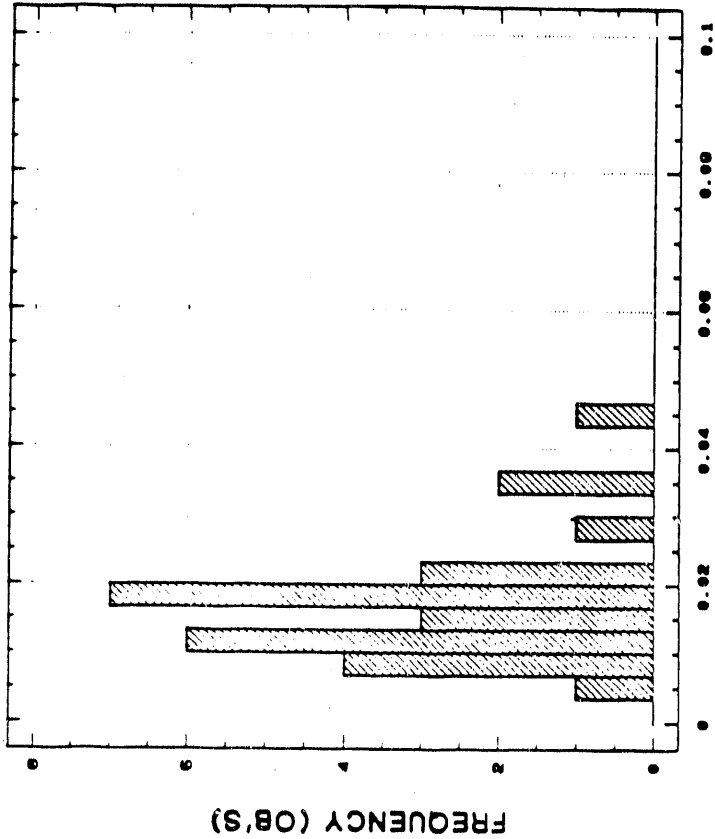
Variable:	HVORSLEV	BOUWER & RICE
Sample size	28	28
Average	0.0284107	0.0175357
Median	0.0245	0.0165
Standard deviation	0.0202392	8.94001E-3
Minimum	8.1E-3	6.5E-3
Maximum	0.1	0.044
Range	0.0919	0.0375

TO CONVERT FROM METERS/DAY (m/d) TO FEET/DAY (ft/d) MULTIPLY BY 3.28

FREQUENCY HISTOGRAM AND SUMMARY STATISTICS FOR OBSERVATION WELLS (METERS/DAY)		
	FIGURE 6-4	
REPORT NO: DOE/OR/21548-122	DRAWING NO.: A/PI/018/0590	
ORIGINATOR: JDC	DRAWN BY: GLN	DATE: 5/90
	GLN	

Values for test data analyzed by the Bouwer and Rice method
are generally lower than values determined by the Hvorslev
method. This is because the Hvorslev method assumes that the
effective radius of influence for the test (i.e. the radius over
which head loss or gain is dissipated) is equal to the distance
from the bottom of the well to the potentiometric surface.
Bouwer and Rice determined a method of calculating the effective
radius of influence, R_e, from equation (1) based on an electrical
resistance network analog for different test geometries with the
assumption that drawdown of the water table around the well is
negligible, that capillary drainage can be ignored, head losses
as water enters the well (well losses) are negligible, and the
aquifer is homogeneous and isotropic (Bouwer and Rice 1976).
With this in mind, the Bouwer and Rice method was used to analyze
all data because it is considered to more closely simulate test
conditions. The Hvorslev technique was also used because it is
widely used, hence levels itself to comparisons with other data.

Analysis of slug test recovery data using the Bouwer and Rice
Method was performed in general accordance with guidance supplied
by Bouwer and Rice (1976) and Bouwer (1989). However, late time
data was included in many cases so that it may appear that the
data are not being treated in the manner prescribed by Bouwer and
Rice, who suggest using straight line portions of the data which,
in the examples, are displayed in early portions of the head
recovery curve.

It should be noted that the examples in the literature are
based on alluvial aquifer conditions where recovery occurs
relatively rapidly, while conditions beneath the Weldon Spring
site (WSS) more closely resemble aquitard properties in many
instances. Almost all data exhibited fairly rapid early time
recovery, which is considered to be indicative of filterpack or

annular influence. Future tests could use a potable water slug in order to minimize the effect of annular influence on recovery data. A water slug could be used to perform a falling head test by filling the well to the top of the casing with potable water. The active head would then be on the order of tens of feet rather than 2 to 5 feet. The larger active head would effectively exceed annular influence capacity (filterpack, developed zone), whereas most of the smaller active head (induced by relatively small solid slugs) is rapidly transmitted to the higher permeability filterpack and developed zone.

Figure 6-5 is a plot of the depth of the screened (mid-screen) interval below the top of bedrock on the vertical axis and hydraulic conductivity values increasing to the right on the horizontal axis. Plotted values are from all wells and were analyzed using the Bouwer and Rice method. The plot does not indicate any observable trend in hydraulic conductivity with respect to the depth of the screened interval below the top of bedrock. Hydraulic conductivity for MW-3006, one of the deepest wells tested, was significantly greater than the average and is probably a result of water-filled fractures at depth, as noted on the drilling log. Geochemical and contaminant data may be useful in determining whether water in this well is more like water in shallow wells than water in other deep wells.

While the lack of an observable trend with respect to the vertical distribution of hydraulic conductivity may seem to conflict with previous observations regarding a general decrease in hydraulic conductivity with increasing depth (BNI 1987), it should be noted that Bechtel conducted borehole permeability testing of both the unsaturated and saturated portions of the Burlington-Keokuk. It is well documented that the upper highly

DEPTH OF SCREEN BELOW TOP OF BEDROCK
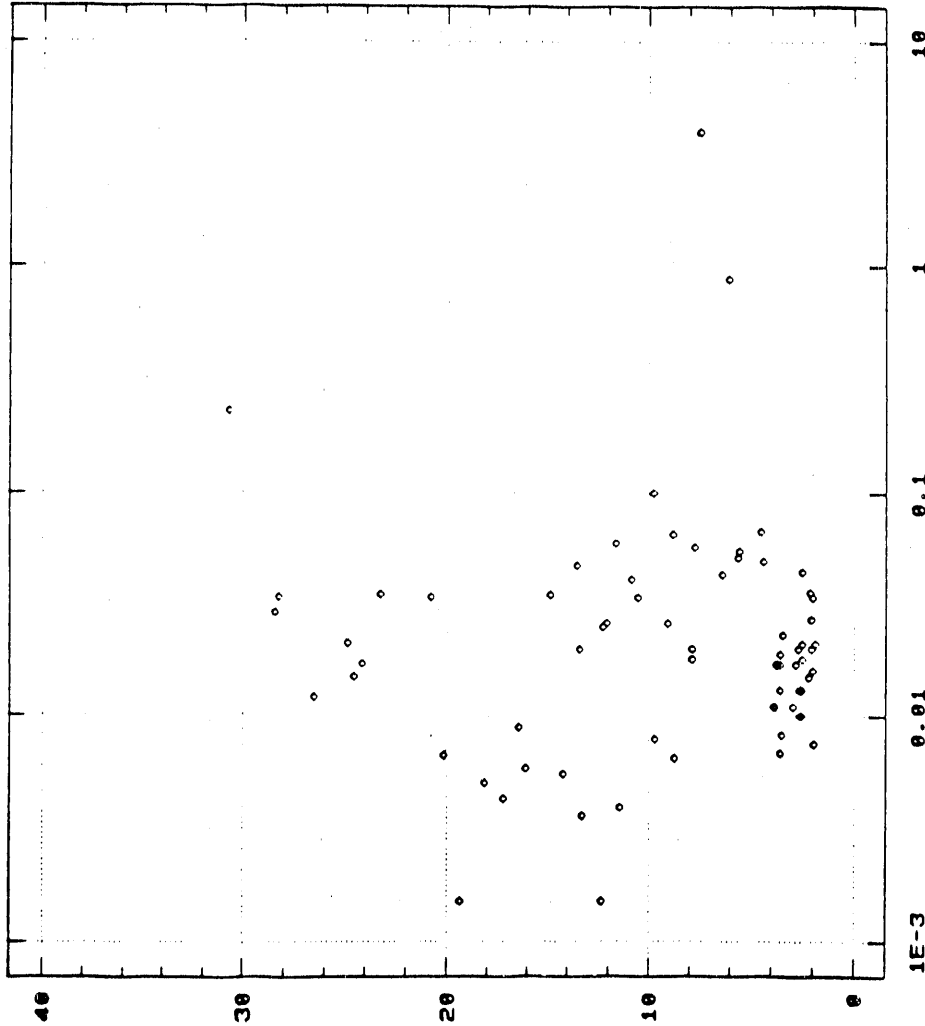
HYDRAULIC CONDUCTIVITY (m/d)

DISTRIBUTION PLOT OF HYDRAULIC
CONDUCTIVITY VALUES VERSUS DEPTH
OF SCREEN BELOW TOP OF BEDROCK
(HYDRAULIC CONDUCTIVITY VALUES ARE
BOUWER & RICE METHOD)

FIGURE 6-5

REPORT NO.: DOE/OR/21548-122	DRAWING NO.: A/PI/018/0590
ORIGINATOR JDC	DRAWN BY: GLN	DATE: 5/90

TO CONVERT FROM METERS/DAY (m/d) TO
FEET/DAY (ft/d) MULTIPLY BY 3.28

weathered portion of the bedrock is a zone of poor core recovery and frequent drilling fluid loss which is indicative of highly porous material (MKF and JEG 1990). However, this portion of the bedrock is generally not included in the slug test data due to the usually unsaturated nature of the high porosity zones. Possible exceptions to this are GT-58P and MW-4014, which are considered to reflect saturated conditions within the weathered bedrock. The values for these wells compare favorably with values reported by Bechtel for the unsaturated bedrock.

Drilling logs from these locations note loss of circulation, bit drop, and core loss during drilling. MW-4014 was injected with one pound of pyranine on July 1, 1988 as part of the Missouri Department of Natural Resources (MDNR) dye tracing program. The tracer was not detected at any of the sampling locations as of December 1988. However, the amount of dye used for the injection may have been insufficient to produce a positive detection. Based on slug test results as well as core loss, fluid loss during drilling, and quick recovery during development and purging for groundwater sampling, the hydraulic conductivities of these wells are considered to be typical of saturated portions of the upper weathered Burlington-Keokuk Limestone.

Slug test values for the observation well networks did not reveal any heterogeneities such as those discussed above. This is probably due to the fact that the highly weathered upper portion of the Burlington-Keokuk is not saturated in the vicinity of the observation well networks. Results of pumping conducted at the PW-3 network suggest that OB3I may not be functional due to lack of drawdown. However, slug tests performed on this well did not indicate poor hydraulic function of the well.

6.2 Pumping Tests

The following subsections present the results of pumping test data analyses. Transmissivity and storativity were determined using the Cooper-Jacob method. The Hantush method was used to determine anisotropy, transmissivity, and storativity. Additionally, hydraulic conductivity was calculated from pumping test data for correlation with slug test results.

6.2.1 PW-1 Results

All of the observation wells in the PW-1 network responded to pumping of PW-1. Data from these wells and PW-1 provided 10 sets of data for analysis. Figure 6-6 shows a summary of these results.

The values of transmissivity and storativity that were obtained using the Cooper-Jacob method are presented in Table 6-3. The values of transmissivity range from 3.6E-02 m²/d (2.9 gpd/ft) to 5.8E-01 m²/d (46.6 gpd/ft) with a mean of 2.0E-01 m²/d (16.3 gpd/ft) and storativity values range from 1E-4 to 6.8E-04 with a mean of 2.9E-4. The Hantush method provided maximum and minimum values of transmissivity around PW-1 equal to 3.5E-01 m²/d (28.4 gpd/ft) and 1.8E-01 m²/d (14.4 gpd/ft), respectively, and a mean storativity of 1.7E-4.

Analysis using the Hantush method indicates the maximum transmissivity has a bearing of approximately N72°W. Comparingthe maximum and minimum transmissivities, it is apparent that the anisotropy ratio is approximately 2:1.

PW1 TRANSMISSIVITY ELLIPSE

PW2 TRANSMISSIVITY ELLIPSE

PW3 TRANSMISSIVITY ELLIPSE

FROG POND

ASH POND

RAFFINATE PITS

N72°W

N10°W

N12°E

MW-2012
MW-2013
MW-2006
MW-2010
MW-2011
MW-2016
MW-2015
MW-2007
MW-2005
MW-2001
MW-2002
MW-2003
MW-3003
MW-2016

$T_{max} = 0.35 m^2/d$
$T_{min} = 0.18 m^2/d$
$S = 3.6E-4$
Principal Anisotropy 2:1 N72°W

$T_{max} = 0.90 m^2/d$
$T_{min} = 0.25 m^2/d$
$S = 1.1E-3$
Principal Anisotropy 3.6:1 N10°E

$T_{max} = 0.30 m^2/d$
$T_{min} = 0.18 m^2/d$
$S = 3.6E-4$
Principal Anisotropy 2:1 N12°E
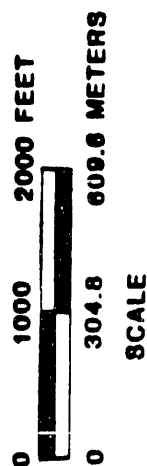
TO CONVERT SQUARE
METERS/DAY (m^2/d) TO
GALLONS/DAY/FOOT (gpd/ft)
MULTIPLY BY 80.5

■ PUMPING WELL
● OBSERVATION WELL
▲ MONITORING WELL

SCALE

| 0 | 1000 | 2000 FEET |
| 0 | 304.8 | 609.6 METERS |

SUMMARY OF PUMPING TEST RESULTS

FIGURE 6-6

REPORT NO.: DOE/OR/21548-122   DRAWING NO.: A/CP/008/0590

ORIGINATOR JDC   DRAWN BY GLN   DATE: 5/90

TABLE 6-3 Hydraulic Properties Determined from Pumping Tests (Cooper Jacob Method)

Well	Pumping Data T* (m²/d)	K** (m/d)	S	Recovery Data T (m²/d)	K (m/d)	S
PW-1	0.078	0.0064		0.036	0.0030	
OB1A	0.19	0.016	0.00036	0.098	0.0080	0.00061
OB1B	0.30	0.025	0.00013	0.13	0.011	0.00020
OB1C	0.48	0.039	0.00013	0.26	0.021	0.00016
OB1D	0.19	0.016	0.00053	0.10	0.0082	0.00057
OB1E	0.31	0.025	0.00025	0.16	0.014	0.00026
OB1F	0.58	0.048	0.00018	0.31	0.025	0.00023
OB1G	0.20	0.017	0.00043	0.09	0.0078	0.00068
OB1H	0.23	0.019	0.00014	0.14	0.011	0.00018
OB1I	0.27	0.022	0.00010	0.14	0.011	0.00011
PW-2	0.11	0.0093		0.028	0.0023	
OB2A	0.42	0.035	0.00083	0.29	0.024	0.00116
OB2B	0.77	0.063	0.00158	0.65	0.054	0.00092
OB2C	0.94	0.077	0.00091	0.69	0.057	0.00047
OB2D	0.42	0.035	0.00081	0.20	0.016	0.00079
OB2E	0.62	0.051	0.00034	0.30	0.025	0.00033
OB2F	0.87	0.071	0.00043	0.57	0.047	0.00034
OB2G	0.41	0.034	0.00183	0.23	0.019	0.00101
OB2H	0.67	0.055	0.00102	0.47	0.038	0.00046
OB2I	0.69	0.057	0.00101	0.55	0.045	0.00040
OB2J	DID NOT RESPOND TO PUMPING					
PW-3	0.057	0.0047		0.032	0.0026	
OB3A	0.21	0.018	0.00054	0.11	0.0095	0.00052
OB3B	0.27	0.022	0.00023	0.18	0.015	0.00025
OB3C	0.31	0.026	0.00015	0.21	0.017	0.00017
OB3D	0.21	0.017	0.00055	0.10	0.0087	0.00070
OB3E	0.25	0.021	0.00015	0.13	0.011	0.00026
OB3F	0.37	0.031	0.00014	0.16	0.013	0.00018
OB3G	0.27	0.022	0.00046	0.13	0.011	0.00102
OB3H	0.30	0.025	0.00014	0.14	0.012	0.00028
OB3I	DID NOT RESPOND TO PUMPING					

T - Transmissivity
K - Hydraulic Conductivity
S - Storativity
* To convert transmissivity values from square meters per day (m²/d) to gallons per day per foot (gpd/ft) multiply by 80.5.
** To convert hydraulic conductivity from meters per day (m/d) to feet per day (ft/d) multiply by 3.28.

Hydraulic conductivity values calculated from pumping and recovery data for the PW-1 array averaged 2.3E-02 m/d and 1.2E-02 m/d respectively.

6.2.2 PW-2 Results

Nine of the observation wells in the PW-2 network responded to the pumping of PW-2. Data from these wells and PW-2 provided 10 sets of data for analysis. Figure 6-6 summarizes these results. Deep observation well OB-2J (screened from 39.6-42.7 m [130-140 ft.]), at the PW-2 array did not respond to the pumping of PW-2.

The values of transmissivity and storativity obtained using the Cooper-Jacobs method are presented in Table 6-3. The values of transmissivity range from 2.8E-02 m²/d (2.3 gpd/ft) to 8.7E-01 m²/d (70.4 gpd/ft) with a mean of 4.9E-01 m²/d (39.9 gpd/ft) and storativity values range from 3.3E-4 to 1.8E-3 with a mean of 8.1E-4. The Hantush method provided maximum and minimum values of transmissivity around PW-2 equal to 9.0E-01 m²/d (72.4 gpd/ft) and 2.5E-01 m²/d (20.5 gpd/ft), respectively, and an overall storativity of 1.3E-3.

Analyses using the Hantush method indicate the maximum transmissivity has a bearing of approximately N101°W. Comparing the maximum and minimum transmissivities, it is apparent that the anisotropy ratio is approximately 3.5:1.

Hydraulic conductivity values calculated from pumping and recovery data using the pumping and observation wells at the PW-2 location averaged 4.9E-02 m/d for pumping data and 3.3E-02 m/d for recovery data.

6.2.3 PW-3 Results

Eight of the nine observation wells at the PW-3 network responded to the pumping of PW-3. Data from these wells and PW-3 provided nine sets of data for analysis. A summary of results is presented in Figure 6-6. OB-3I did not show any response to the pumping of PW-3. A discussion of possible explanations for the lack of response at OB-3I is presented in Subsection 6.2.4.1.

The Cooper-Jacob analysis of the data from the PW-3 array provided many values of transmissivity and storativity (Table 6-3). The values of transmissivity range from $3.2E-02$ m^2/d (2.6 gpd/ft) to $3.7E-01$ m^2/d (29.9 gpd/ft) with a mean of $1.9E-01$ m^2/d (15.5 gpd/ft) and storativity values range from $1.4E-4$ to $1.0E-3$, with a mean of $3.6E-4$. The Hantush method provided maximum and minimum values of transmissivity around PW-3 equal to $3.0E-01$ m^2/d (24.3 gpd/ft) and $1.8E-01$ m^2/d (14.4 gpd/ft), respectively, and an overall storativity of $4.0E-4$.

Analyses using the Hantush method indicate the maximum transmissivity has a bearing of approximately N12°E. Comparing the maximum and minimum transmissivities, it is apparent that the anisotropy ratio is approximately 2:1.

Hydraulic conductivity values calculated from pumping and recovery data using pumping and observation wells at the PW-3 locations averaged $2.1E-02$ m/d for pumping data and $1.1E-02$ m/d for recovery data.

6.2.4 Discussion

6.2.4.1 Pumping Test Data

The results of pumping test data analyses can be most readily compared by referring to Figure 6-6. Figure 6-6 shows that the major axis of transmissivity is aligned approximately north-south at the PW-2 and PW-3 networks. However, the effective transmissivity at PW-2 is approximately twice that for the vicinity of PW-3. Furthermore, the degree of anisotropy is greater near PW-2 than PW-3 and storativity was determined to be an order of magnitude higher near PW-2. Higher hydraulic properties for the PW-2 vicinity may be attributed to the fact that the PW-2 network is screened higher in the section and monitors a more highly weathered portion of the Burlington-Keokuk. Comparison of PW-2 results with those for PW-1 and PW-3 may indicate vertical anisotropy within the upper Burlington-Keokuk Limestone.

Figure 6-6 also shows that the major direction of anisotropy near PW-1 is aligned approximately parallel to the northwest trending observation well array, approximately 60° from the orientation of maximum transmissivity at PW-2 and PW-3. Note that the major axis of the apparent transmissivity tensor at PW-3 is oriented approximately parallel to the minor axis at PW-1. Also the values for transmissivity and storativity near wells PW-1 and PW-3 are approximately equal.

As noted previously, the current analyses have concentrated on observing and interpreting effects of lateral anisotropy. However, evidence of other phenomena has been observed in the test well data. Although quantification of such phenomena is

hindered by the quality of the data, the following statements can be made about some of the apparent phenomena:

o In general, the pumping test data were reviewed for evidence of short-term or long-term recharge effects, barrier-boundary effects, and hydraulic separation between pumped wells and observation wells.

o Although the data from wells near PW-1 showed evidence of recharge effects, as evidenced by declining rates of drawdown during the test, they also show increasing rates of drawdown during latter stages of the test. The variations in drawdown do not correlate to similar variations in pumping rates, indicating a likelihood of other hydraulic phenomena occurring. One possible explanation of the phenomenon would be classical delayed yield due to gravity drainage. This interpretation would be consistent with the very low values of storativity (1E-04 to 1E-03) calculated from earlier portions of the time-drawdown data, before the recharge effects began to be observed. However, the changes from declining to increasing rates of drawdown were generally more abrupt than would be expected from classical delayed yield effects, and the phenomena are not consistently observed for all three pumping well locations. An alternative interpretation might be recharge derived from draining a larger fracture or conduit near the pumping well, followed by barrier-boundary effects once the fracture has been locally drained.

For the vicinity of PW-2, recharge effects are generally observed only along the south-bearing ray of wells. This is also the approximate orientation of the major direction of

transmissivity. Along the other two rays, recharge effects are generally not observed, whereas barrier effects are definitely observed at two wells and possibly observed at two other wells. These results suggest that delayed yield may be due to a zone of discrete flow which parallels the south-bearing ray of wells. These results are consistent with possible recharge from fractures or conduits along the south-bearing ray, with no such features along the northwest- and northeast-bearing rays.

The fact that OB2J did not respond to pumping, yet lies along the principal axis of anisotropy, suggests that discrete flow influences present along the south-bearing ray do not extend to the depth of the screened interval of OB2J.

In the vicinity of PW-3, recharge effects are commonly observed and evidence of late time barrier effects is lacking. This again suggests that delayed yield is not a predominant phenomenon. This effect would, however, be consistent with more generalized dual-permeability conditions near PW-3. In this interpretation, diffuse-flow permeability, which is reflected in the calculated aquifer parameters, would provide the major response of the aquifer to pumping, with discrete-flow permeability providing generalized recharge later in the test. The diffuse-flow permeability could be attributed to intergranular or fine-fracture flow, with discrete-flow permeability resulting from larger, more widely spaced fractures or conduits.

In addition to the potential recharge effects described above there is also some evidence of short-term effects consistent with a dual-permeability aquifer. In data from several wells, there was a short-time rise in water levels, or brief flattening of the drawdown curve, which would be consistent with temporary recharge

from a fracture or conduit, followed by cessation of recharge consistent with drainage of the fracture. Such effects are seen in wells PW-1 (500 minutes), OB1A and OB1G (200-350 minutes), and possibly OB1I (400-500 minutes); note that wells OB1A and OB1G are aligned approximately parallel to the inferred major direction of anisotropy at PW-1. Since such effects are seen in all nine observation wells, this may partially explain the generally higher transmissivities and storativities inferred from data at PW-2 than from the other two wells. Similar short-term recharge effects are not readily observed in data from PW-3 observation wells indicating that the cone of influence for PW-3 is dominated by diffuse flow permeability.

Isolated evidence of barrier-boundary effects was also occasionally observed, notably in wells OB2C, OB2G, and OB3F, and possibly in test wells PW-2 and PW-3. Wells OB2C, OB2G, and PW-2 are aligned generally parallel to the direction of minimum transmissivity near PW-2 indicating a lack of discrete-flow permeability along this orientation.

Two observation wells did not readily respond to production from nearby pumping wells: OB2J and OB3I. OB3I is located about 18 m (60 ft) from PW-3 along ray 3, and is screened at an elevation comparable to that of PW-3. Slug test data indicate that OB3I responds in a manner similar to other observation wells near PW-3, so it does not appear to be hydraulically isolated due to any well construction or well development difficulties. A possible explanation could be the presence of a filled fracture (as have been observed during site drilling activities) lying between OB3H and OB3I. However, no boundary effects were seen in the drawdown curve of OB3H.

Well OB2J is located approximately 6 m (19 ft) from PW-2, but
is screened within a much deeper interval of the limestone 40-43
m (130-140 ft) below ground surface for OB2J compared to
approximately 14-26 m (45-85 ft) below ground surface for the
other observation wells at PW-2). The lack of response at this
well suggests a degree of hydraulic separation between shallower
and deeper parts of the aquifer, consistent with the results of
in situ aquifer tests and water-level observations. The
hydraulic separation may be due to strong vertical anisotropy due
to the layered nature of the aquifer, a general decline in
hydraulic conductivity with depth due to smaller apertures and
more widely spaced fractures, or a combination of such factors.

The drawdown data were reasonably consistent with the
constraints of the Hantush approach for analyzing data in the
presence of areal anisotropy. It was possible to readily match
the observed drawdown distributions with families of ellipses
having more-or-less parallel major and minor axes. Furthermore,
it was generally possible to obtain reasonably consistent
transmissivity estimates from different observation wells
utilizing different analytical techniques (Jacob time-drawdown,
Hantush time-drawdown, Jacob distance-drawdown, and Hantush
distance-drawdown). Exceptions to this general conclusion are
discussed above.

In general, many of the observation wells exhibited evidence
of significant recharge in the later portion of the tests. This
is consistent with classical delayed yield due to gravity
drainage, leakage from overlying or underlying beds, or possibly
to double porosity relationships such as could readily occur in a
fractured rock with some degree of intergranular or fine-
fracture porosity. The calculated storativity is relatively low,
consistent with that of a classical confined, homogeneous

aquifer. Since the estimates of storativity are derived largely from early-time data during each test, this low storativity could be consistent with classical delayed yield. Observation wells at PW-1 exhibit some indication of a possible late-time return to a Theis curve, which is also typical of a delayed yield effect. On the other hand, the very-late-time return to an apparent Theis curve is more abrupt than would be expected from classical delayed yield theory. Since this phenomenon is not generally observed at the PW-2 and PW-3 observation wells, delayed yield does not appear to be a major cause of the observed drawdown behavior.

Leakage from overlying or underlying strata is not expected. The pumping and observation wells were designed to be completed in the uppermost saturated interval of the aquifer, so that overlying source beds generally do not exist. Perched groundwater zones are known to exist in the vicinity of the raffinate pits; however, drilling performed for installation of observation wells and pumping wells did not encounter perched conditions. Furthermore, the lack of response at well OB2J suggests that there is relatively little hydraulic connection between the depth interval tested and deeper portions of the Burlington-Keokuk; thus, significant upward leakage is unlikely.

Double porosity effects are quite possible at the site. As noted in previous site reports (MKF and JEG 1989b, BNI 1987), the Burlington-Keokuk Formation is generally expected to exhibit some aspects of both intergranular and fracture porosity. The low transmissivities and storativities observed would be consistent with a very fine-grained, low-permeability granular aquifer, or an aquifer with very fine interconnected fractures which behaves as an equivalent porous medium. The recharge effects would be consistent with secondary fracture porosity zones capable of

supplying recharge to the intergranular aquifer as water levels
are drawn down. There is evidence in the drawdown data from some
observation wells of temporary recharge effects, which might be
consistent with the draining of relatively isolated fracture
zones. There is also evidence in the data from a few wells of
possible barrier-boundary effects, which might suggest poor
lateral communication between wells such as might be expected
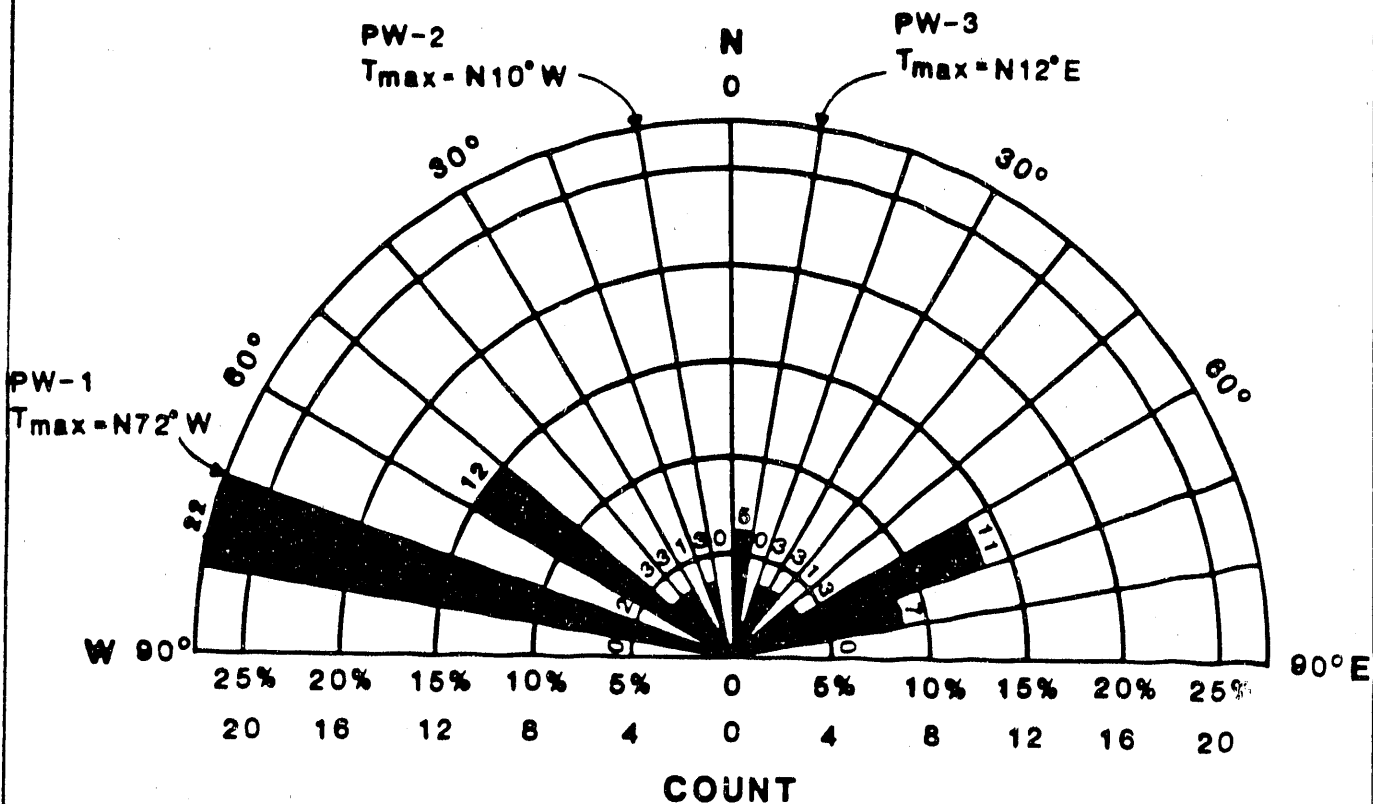under aquitard conditions.

Radii of influence were determined for each of the test
networks (ESI 1989). In general the radii are on the order of 60
m (200 ft). However, along OB1G, OB1H, and OB1I the distance
where zero drawdown occurs is 275 m (900 ft). This ray of wells
lies in the same direction as the primary direction of fractures
in the formation (MKF and JEG 1989b). Therefore, a fracture may
be transmitting the effects of pumping farther than expected.

Hydraulic conductivity values calculated from pumping and
recovery data correlate well with values determined from slug
testing. Table 6-4 presents a comparison of mean hydraulic
conductivity values determined from pumping and observation wells
and slug tests.

Anisotropic analyses of transmissivity indicated orientations
of N72°W for PW-1, N10°W for PW-2 and N12°E for PW-3. In Figure
6-7, the orientations of maximum transmissivity are compared to
fracture orientations observed in bedrock exposures in the
vicinity of the Weldon Spring site. The orientation of maximum
transmissivity at PW-1 coincides with a major fracture set
whereas the orientations of maximum transmissivity at PW-2 and
PW-3 are coincident with minor fracture features. This suggests
that groundwater flow is controlled by lateral anisotropy in the
form of horizontally oriented fractures and that vertical

TABLE 6-4   Comparison of Hydraulic Conductivity Values Determined from
            Slug Tests and Pumping Tests

Pump Well Array	Mean K-Value (m/d) from Pumping Test Data	Mean K-Value (m/d) from Slug Tests (Bouwer and Rice)	Ratio Pumping Test Mean/Slug Test Mean
PW-1	2.3E-02	1.4E-02	1.60
PW-2	4.9E-02	2.1E-02	2.30
PW-3	2.1E-02	1.8E-02	1.20

PW-2
Tmax = N10°W

N
0

PW-3
Tmax = N12°E

PW-1
Tmax = N72°W

30°   30°

60°   60°

W 90°   90° E

25% 20% 15% 10% 5%   0   5%   10% 15% 20% 25%
 20   16   12   8   4   0   4   8   12   16   20

COUNT

A PLOT OF THE STRIKE OF 80 FRACTURES MEASURED
AT BEDROCK EXPOSURES IN THE VICINITY OF THE
WELDON SPRING SITE AND THE ORIENTATION OF
MAXIMUM TRANSMISSIVITY AT PW-1, PW-2 AND PW-3

DIP OF MOST FRACTURES IS NEARLY VERTICAL.

COMPARISON OF WELDON SPRING SITE VICINITY FRACTURE ORIENTATIONS AND ORIENTATIONS OF MAXIMUM TRANSMISSIVITY OF PW-1, PW-2 AND PW-3		
FIGURE 6-7		
REPORT NO. DOE/OR/21546-122	DRAWING NO.: A/PV020/0590	
ORIGINATOR: JDC	DRAWN BY: GLN	DATE: 5/90

fracture orientation has little impact on orientation of lateral anisotropy.

6.2.4.2 Recovery Data

Recovery data were evaluated by the subcontractor, Earth Scientists, Inc. (ESI), using semi-logarithmic plots of elapsed recovery time versus residual drawdown to obtain values of transmissivity and storativity. A verification of the accuracy of the subcontractor recovery results was conducted to determine whether the recovery data warranted reevaluation. The verification process involved construction of time-recovery plots of observation wells to determine storativity values and construction of residual drawdown plots of pumping and observation wells to determine transmissivity. The time-recovery plots and residual drawdown plots were constructed according to Driscoll (1986). Results of the recovery data verification are compared to ESI's reported values in Table 6-5. The verification process did not indicate a significant difference in aquifer property values which could be attributed to the methods of recovery data evaluation.

6.3 Tracer Tests

The following sub subsections present the results of tracer test data analysis. The values obtained from the tracer test data were verified using RESSQ, a two-dimensional advection-adsorption contaminant transport modeling program (Javandel et al. 1984). Values of porosity and induced flow velocity were used to determine a calculated travel time.

Tracer tests were performed at the PW-2 and PW-3 locations which exhibited the upper and lower range, respectively, of

TABLE 6-5 Comparison of Aquifer Properties Determined from Evaluation of
Recovery Data by the PMC and ESI

Well ID	PMC Results		ESI Results	
	Transmissivity*	Storativity	Transmissivity	Storativity
PW-1	0.033	– – –	0.036	– – –
OB1A	0.099	0.00066	0.098	0.00061
OB1B	0.15	0.00027	0.13	0.00020
OB1C	0.26	0.00018	0.26	0.00016
PW-2	0.05	– – –	0.028	– – –
OB2A	0.288	0.00012	0.294	0.00012
OB2B	0.544	0.00092	0.656	0.00092
OB2C	0.650	0.00046	0.690	0.00047
PW-3	0.031	– – –	0.032	– – –

* Square meters/day (m²/d)

To convert from m²/d to gallons per day/foot (gpd/ft) multiply by 80.5.

PMC – Project Management Contractor
ESI – Earth Scientists Incorporated

hydraulic properties determined from pumping tests. Tracer tests 2were not conducted at PW-1 since the hydraulic properties for this location were considered to be similar to those at PW-3.

### 6.3.1 PW-2 Results -- Chloride Tracer

Using Figure 6-8, the tracer centroid arrival time was determined to be 125 hours after injection. Application of Darcy's law yielded an effective porosity of approximately 0.003 in the formation between OB2I and PW-2. Applying the transport equation and the relationship between dispersivity and hydrodynamic dispersion, the dispersivity was found to be approximately 0.049 m (0.16 ft).

6.3.2 PW-2 Results -- Bromide Tracer

Using Figure 6-9, the tracer centroid arrival time was determined to be 260 hours after injection. Application of Darcy's law yielded an effective porosity of approximately 0.015 in the formation between OB2E and PW-2. Applying the transport equation and the relationship between dispersivity and hydrodynamic dispersion, the dispersivity was found to be approximately 0.025 m (0.081 ft).

6.3.3 PW-3 Results -- Chloride Tracer

Using Figure 6-10, the tracer centroid arrival time was determined to be 190 hours after injection. Application of Darcy's law yielded an effective porosity of approximately 0.002 in the formation between OB3F and PW-3. The dispersivity was found to be about 0.014 m (0.047 ft).
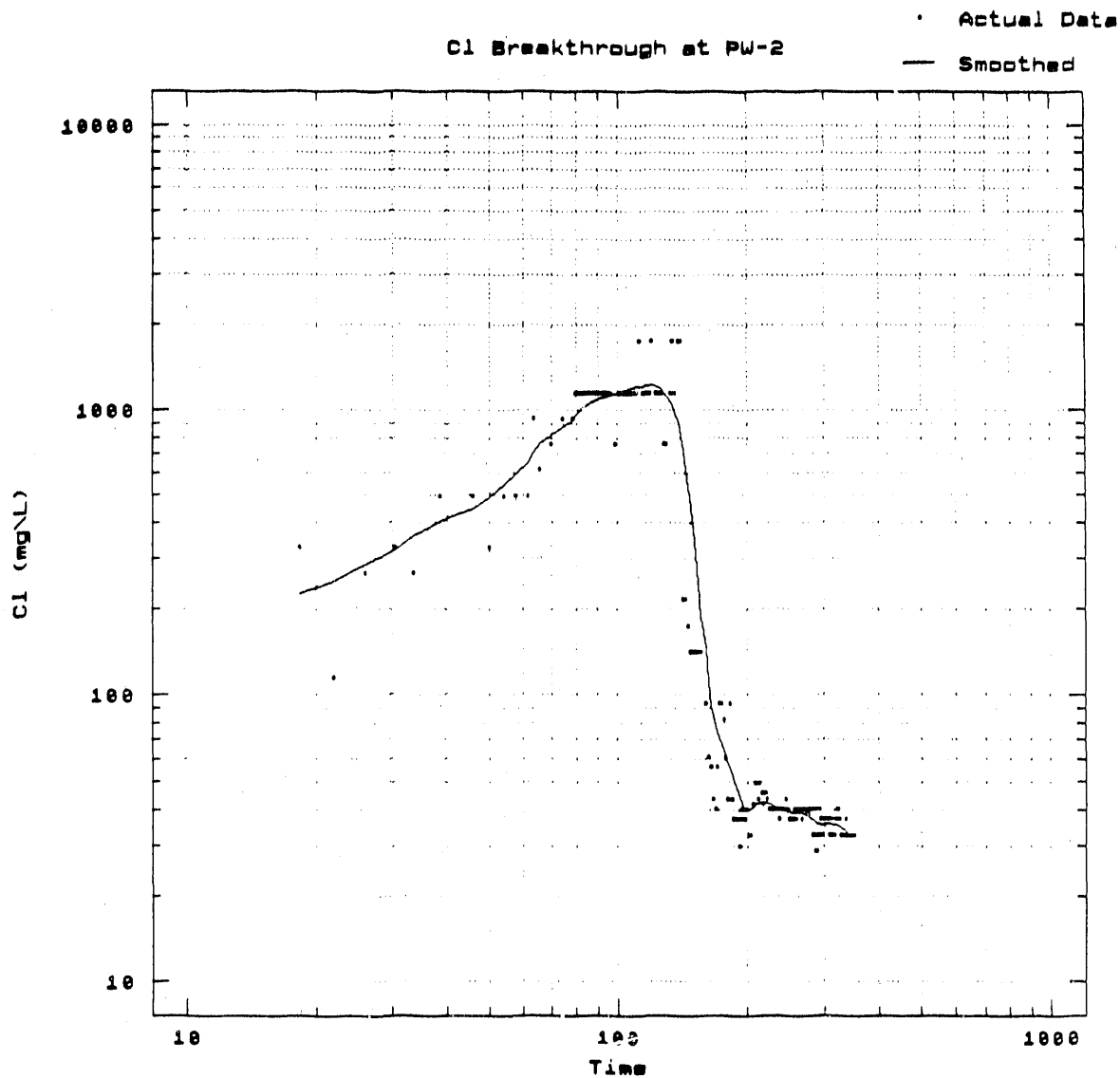
PLOT OF CHLORIDE TRACER
CONCENTRATION VERSUS TIME
AT PW-2

FIGURE 6-8

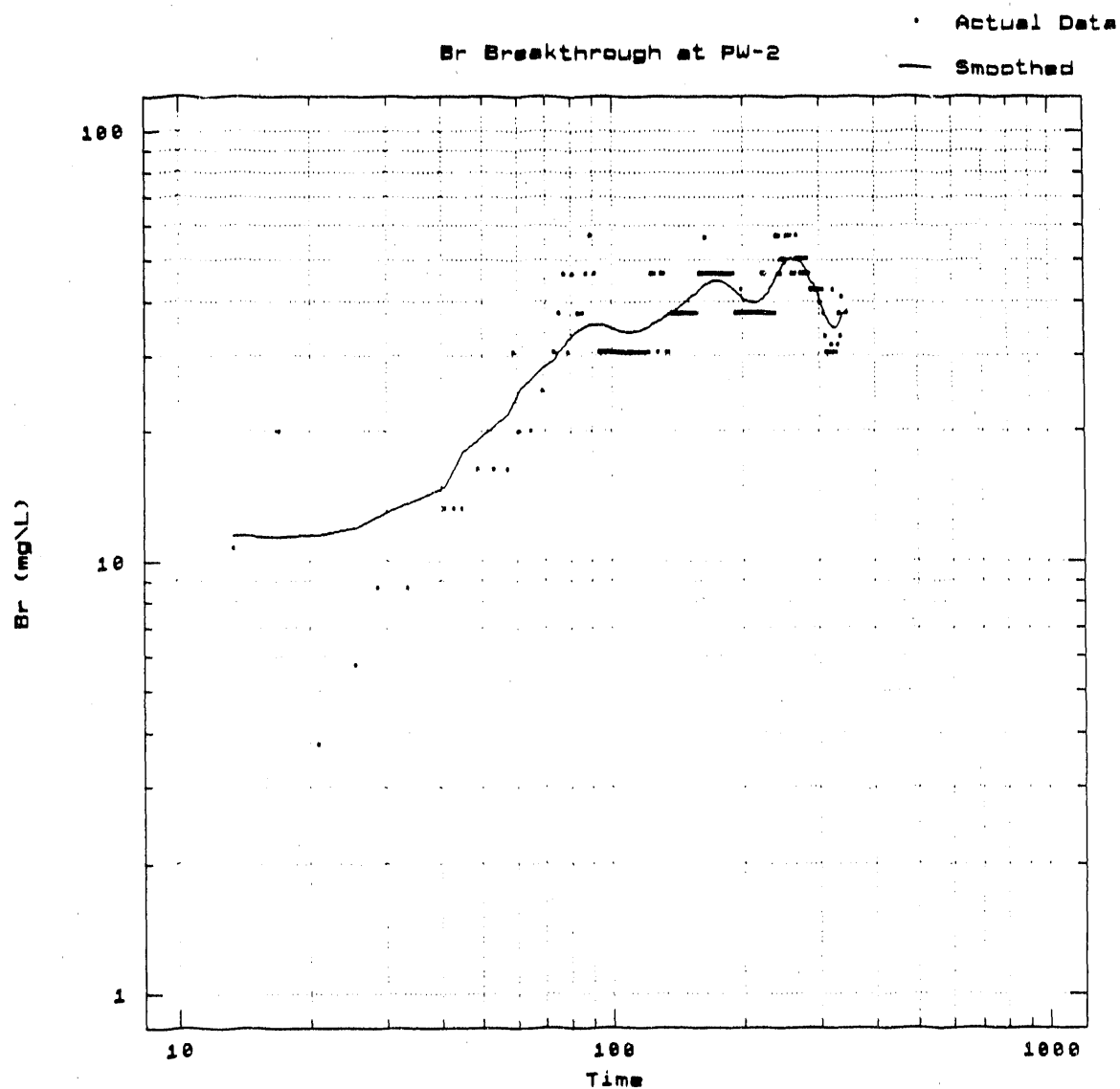Br Breakthrough at PW-2

· Actual Data

— Smoothed

PLOT OF BROMIDE TRACER
CONCENTRATION VERSUS TIME
AT PW-2

FIGURE 6-9

REPORT NO.: DOE/OR/21548-122   DRAWING NO.: A/PV023/0590

ORIGINATOR: JDC   DRAWN BY: GLN   DATE: 5/90
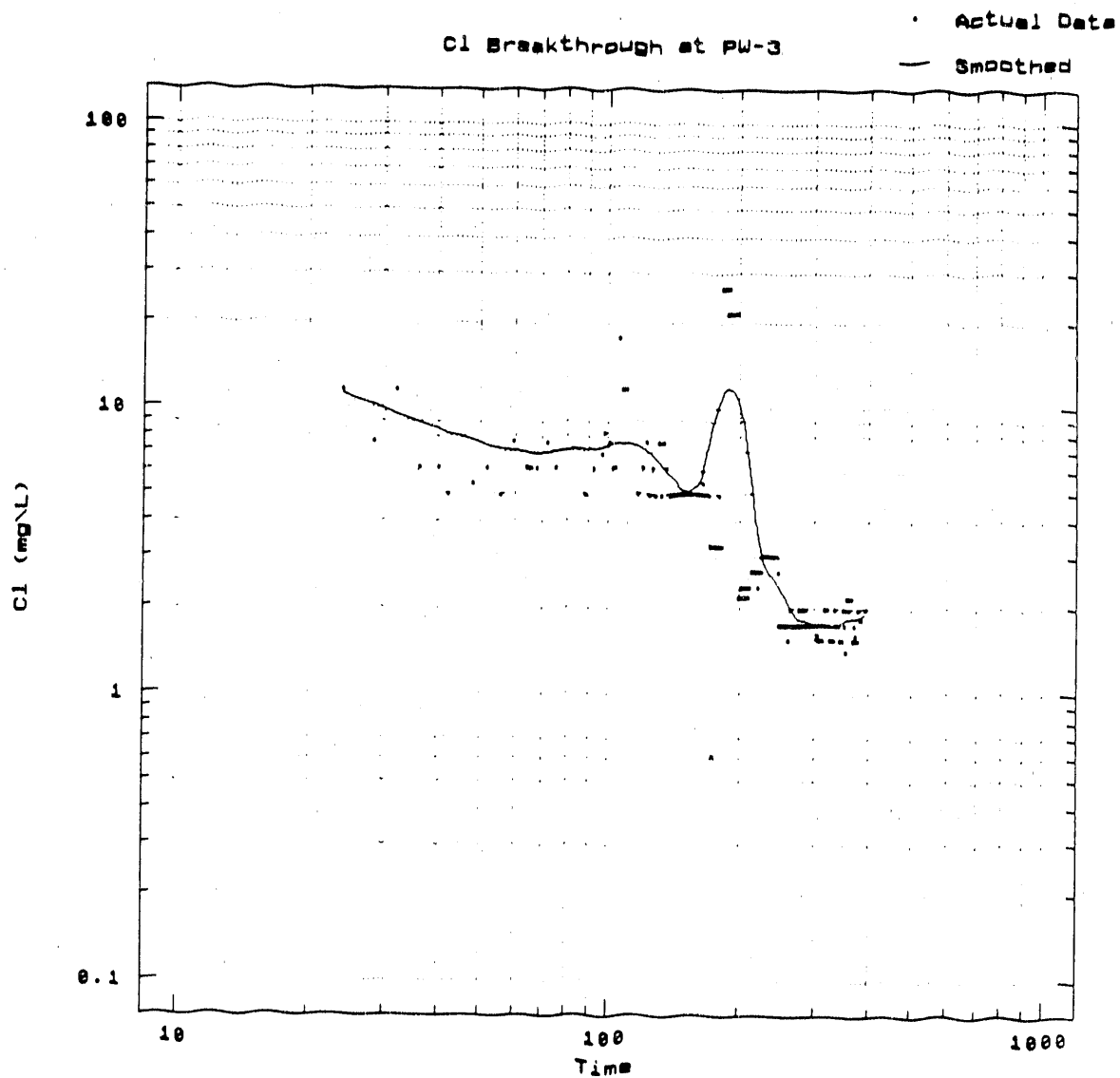
Cl Breakthrough at PW-3

• Actual Data
— Smoothed

PLOT OF CHLORIDE TRACER
CONCENTRATION VERSUS TIME
AT PW-3

FIGURE 6-10

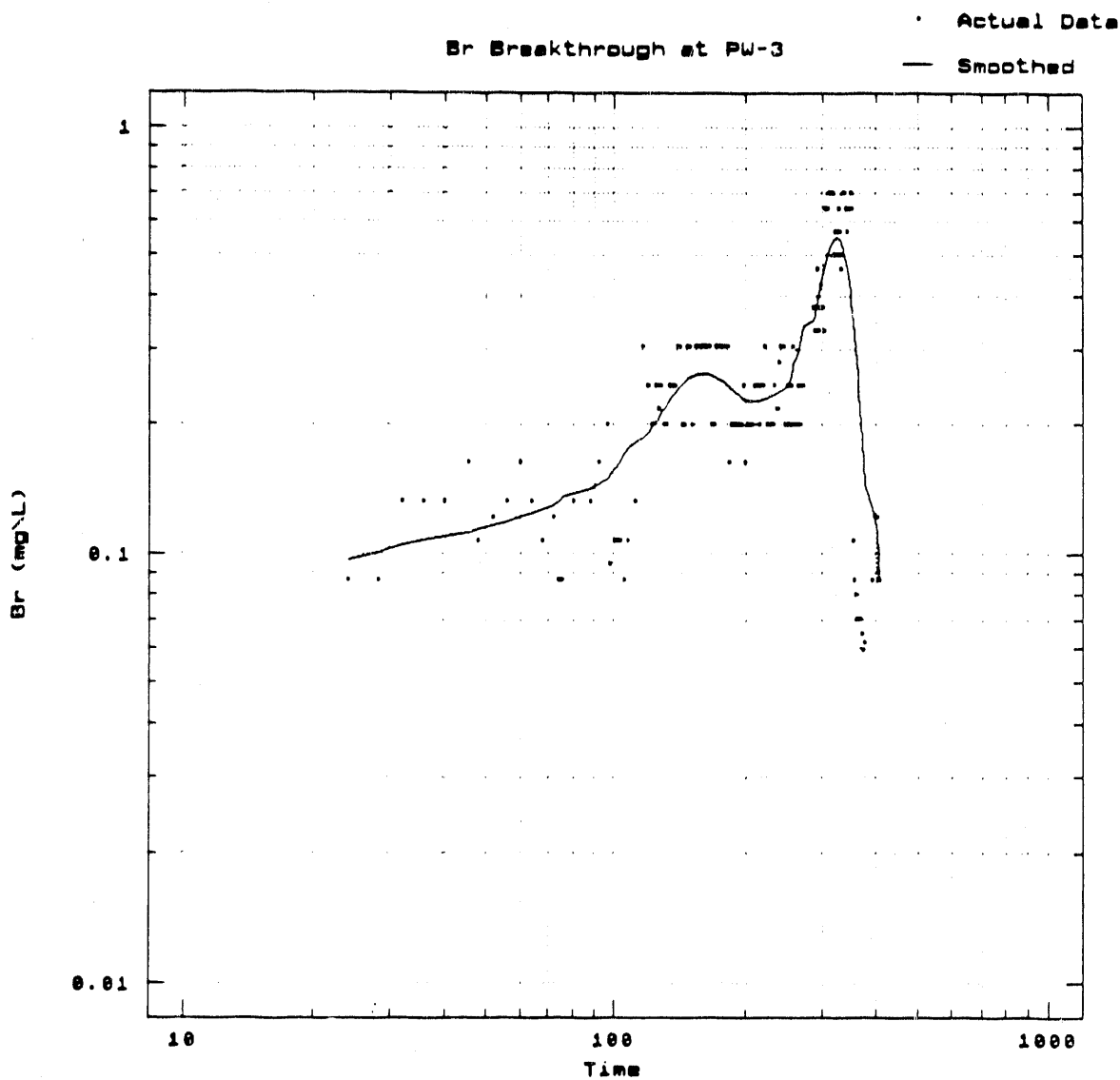| REPORT NO. DOE/OR/21548-122	DRAWING NO. A/PI/024/0590	
ORIGINATOR: JDC	DRAWN BY: GLN	DATE 5/90

6.3.4 PW-3 Results -- Bromide Tracer

Using Figure 6-11, the tracer centroid arrival time was determined to be 320 hours after injection. Application of Darcy's law yielded an effective porosity of approximately 0.006 in the formation between OB3C and PW-3. The dispersivity was found to be about 0.0088 m (0.029 ft).

6.3.5   Discussion

Figures 6-8, 6-9, 6-10, and 6-11 are plots of time versus tracer concentration. A simple moving average technique was used to obtain a smoothed time-series vector for each tracer concentration data set.

The preinjection concentration of chloride at PW-2 was approximately 40 mg/l. From inspection of Figure 6-8 it appears that initial tracer breakthrough occurred prior to sample collection at PW-2. Peak concentration was determined to be at 125 hours. The asymmetric shape indicates dispersion of the tracer front under the induced gradient and a prompt return to preinjection concentrations after arrival of the tracer centroid. The tail dispersion may have been suppressed by the 275 liter chaser used to drive the tracer into the formation. The chaser may have diluted tail concentrations, while accentuating the centroid. The shape of the curve also suggests the tracer behaved as a single slug.

The concentration of bromide with time at PW-2 is shown in Figure 6-9. Preinjection concentrations for bromide were about 0.4 mg/l. While the tracer centroid was determined to have arrived 260 hours after injection, inspection of the data indicates initial breakthrough of peak concentration at

· Actual Data

— Smoothed

Br (mg\L)

1

0.1

0.01

10

100

1000

Time

PLOT OF BROMIDE TRACER
CONCENTRATION VERSUS TIME
AT PW-3

FIGURE 6-11

REPORT NO.: DOE/OR/21548-122	DRAWING NO.: A/PI/025/0590
ORIGINATOR: JDC	DRAWN BY: GLN	DATE 5/90

approximately 88 hours after injection. The 88-hour time value
for bromide breakthrough is not unreasonable considering the
distance necessary for the bromide tracer to travel between OB-2E
and PW-2, compared to the distance necessary for the chloride
tracer to travel between OB-2I and PW-2. Additionally, if the
orientation of maximum transmissivity is considered to be
parallel to the bromide travel path, then a lower breakthrough
time value is expected for the bromide tracer, given that bromide
and chloride have essentially the same degree of
conservativeness. The curve for bromide also exhibits a degree
of oscillation in the centroid which may be the result of
discrete tracer fractions traveling somewhat different travel
paths (fractures), and therefore having different arrival times
due to the relative distance of each travel path. The bromide
concentrations did exhibit a sharp decline as with the chloride
tracer.

Figure 6-10 is a plot of chloride versus time at PW-3. The
preinjection concentration of chloride at PW-3 was about 6 mg/l.
Concentrations of chloride at PW-3 were much lower in general
than those at PW-2. The lower tracer concentrations may be the
result of forcing the tracer into the formation where the bulk of
the tracer entered fracture travel paths which were either of
longer distance than that which could be evaluated with the
available time, or were not connected to flow paths which
intersected the pumping well. Centroid arrival was determined to
be 190 hours after injection. The data also indicate a possible
peak concentration at about 110 hours which may be due to tracer
slug fractionation. Chloride concentrations decline sharply to
below preinjection concentrations beginning at 200 hours and
remain low for the remainder of the monitoring period. The rapid
decline to preinjection levels may be due to dilution by the
chaser water.

Bromide concentrations at PW-3 (Figure 6-11) were also lower than at PW-2. The preinjection bromide concentration was approximately 0.1 mg/l. Dispersion of the tracer front and dilution after the peak concentration is evident on the plot. Bromide also exhibited dual peaks, possibly due to tracer fractionation, similar to what was observed for chloride at PW-3 and bromide at PW-2. Use of the chaser seems to have diluted tail dispersion in a manner similar to what was observed at other locations.

The values of effective porosity obtained from the tracer tests are approximately one order of magnitude higher than the storativity values found from the pumping test data. It is believed that values obtained using the tracer test method are more reliable than values derived from pumping well drawdown data since tracer test values are a result of observed tracer travel times. As with the transmissivity, effective porosity was expected to be low. Results show that it ranges between 0.002 and 0.015. Local variations of the effective porosity, seen around both networks of wells, can be related to the directional variations in lateral anisotropy within the formation as determined by the Hantush analysis of pumping test data.

Dispersivity is a measure of the amount of mechanical mixing that occurs in a contaminant mass as it travels through a porous media. Causes of mixing include velocity differences within the pores and differences in the length of the pore channels through which the contaminant molecules move. Mixing causes some of the contaminant molecules to travel faster and some slower than the average linear groundwater velocity. Therefore, dispersivity causes the contaminant plume to grow in size as time increases. Dispersivities ranging from a minimum of 0.0088 m (0.029 ft) to a maximum of 0.049 m (0.16 ft) were determined from the tracer test

data. These values are relatively low and may indicate that a
contaminant plume in the aquifer would increase in size very
slowly. Correspondingly, contaminant concentrations may
decrease, assuming that retardation mechanisms are negligible.
The low values also indicate that the tested portions of the
aquifer can, in a general sense, be treated as an equivalent
porous medium since lower values would be indicative of fracture
flow with less mixing.

Field-scale dispersivities are also considered to be
proportional to the scale of the transport path under
investigation (Fetter 1980). Since the tracer tests were applied
to a rather small portion of the aquifer volume it is implicit
that observed dispersivity values are smaller than what would be
observed during a larger-scale test in more porous media.
Consequently, it is difficult to make substantive inferences
regarding the relative magnitudes of intergranular and fracture
flow based solely on tracer test data. From inspection of tracer
tests, it was determined that secondary porosity effects are
evident as pulses in tracer concentration due to differential
velocity through fractures. In the test horizon, primary
porosity (intergranular) is considered to be very low while
secondary porosity can be expected to exhibit a range of values.
The lower end of this range is represented by tracer test data
obtained during pumping. The upper end is represented by high
slug test values (MW-4014 and GT-58P).

In order to increase confidence in the values for effective
porosity derived from the tracer tests, the advection-adsorption
contaminant transport model RESSQ was used to simulate tracer
transport and verify initial arrival times of the tracers. RESSQ
is normally used to simulate both contaminant transport from
sources (e.g., injection wells, leaky tanks, or impoundments) to

sinks (e.g., extraction wells or natural groundwater discharge locations) and variations in contaminant concentrations with time. However, the program is considered applicable for verification of tracer travel times where the observation wells used for tracer injection are considered to represent sources and the pumped wells represent concentration sinks.

RESSQ was run for each tracer test using the effective porosities derived from each test. These values are reported in Section 6.3. Additional parameters required to run RESSQ include flow direction (which in this case was the bearing between the observation well used for tracer injection and the pumped well), average linear velocity due to pumping, aquifer thickness, and the adsorption capacity of the host media. Average linear velocity due to pumping ranged from 7.8E-03 m/day (2.5E-02 ft/day) for the chloride tracer traveling between OB-3F and PW-3, to 2.5E-02 m/day (8.2E-02 ft/day) for the bromide tracer traveling between OB-2E and PW-2. Aquifer thickness was assumed to be 12.5 m (41 ft) for all cases and adsorption capacity was considered to be zero for all cases.

Travel times determined using RESSQ ranged from 16 to 45 days, while actual travel times ranged from 8 to 10 days.

The differences in the range of observed tracer travel times and those determined using RESSQ are considered to be sufficiently small with respect to the validity of tracer-derived values for effective porosity. This is demonstrated by the observation that input porosity values for RESSQ would only decrease by a factor of four in order to obtain an RESSQ travel time equal to that seen in the tracer tests.

7 FLOW DYNAMICS

This section presents determinations of hydraulic gradients and calculations of groundwater velocities for selected flow paths using input values based on the results of slug tests and tracer tests.

7.1 Hydraulic Gradients

Horizontal hydraulic gradients were determined for six potential flow paths, four in the shallower portion of the Burlington-Keokuk Limestone and two in the deeper portion of the same formation. Flow paths were chosen to obtain values for average linear groundwater flow velocity under diffuse Darcian conditions. The horizontal flow paths were chosen to obtain a range of values for flow in a number of directions. The choice of deep flow paths is limited directionally due to the distribution of deep wells at the site. The selected flow paths do not suggest preferred flow paths. For horizontal flow situations, the hydraulic gradient is a measure of the slope of the potentiometric surface of the groundwater within an aquifer. It is defined as:

$$i = \frac{dh}{dl}$$

(13)

where:

dh = difference in potentiometric head between two points

dl = distance between the two points.

The gradients that were obtained along the selected flow paths are presented in Table 7-1.

The vertical flow component has been inferred to be very low. The Phase II Groundwater Quality Assessment for the Weldon Spring Chemical Plant, Raffinate Pits and Vicinity Properties (MKF and JEG 1989a) suggests that there is poor communication between the upper and lower portions of the aquifer. This inference is based on vertical distributions of contaminants. Also, results of the pumping test at the PW-2 network showed that OB2J did not respond to pumping. This indicated that there is little or no communication between the upper (weathered) and lower (competent) portions of the aquifer.

Observed hydraulic gradients at well pairs exhibited a range of values from approximately 0.6 for MW-2018 and MW-2019 to 0.009 for MW-3006 and MW-3003. This range of observed gradients, along with the lack of response in OB2J during pumping, probably reflects the limitations of an equivalent porous medium approach, where diffuse flow, occurring within fine fractures, and a strong horizontal anisotropy inhibit vertical flow which can be assessed through Darcian principles. Some variation in vertical gradient may be due to the relative proximity of the various well pairs to widely spaced vertical fractures. Distributions of contaminant levels in paired deep and shallow wells do not correlate well with values of observed hydraulic gradients. For example, the vertical gradient between MW-3003 and MW-3006 is 0.009, which suggests relatively good hydraulic communication. However, nitrate concentrations reported in the 1989 Annual Site Environmental Report (MKF and JEG 1990b) ranged from 312,000 mg/l to 1,885 mg/l for MW-3003. The range for nitrate in MW-3006 during the same time period was 188.0 mg/l to undetected which,

TABLE 7-1 Hydraulic Gradients and Hydraulic Conductivities and Resulting Average Linear Velocities of Groundwater

Flow Path	Hydraulic Gradient	Hydraulic Conductivity (m/d)		Average Linear Velocity (m/d) *	
		Bouwer and Rice	Hvorslev	Bouwer and Rice	Hvorslev
MW-3003 to MW-2002	7.5E-03	2.5E-02	6.3E-02	2.9E-02	6.8E-02
MW-2013 TO MW-4017	1.6E-02	3.3E-02	6.6E-02	7.6E-02	1.5E-01
OB2F TO MW-4021	5.0E-03	3.1E-02	4.6E-02	2.2E-02	3.3E-02
MW-2018 TO MW-4022	2.2E-02	3.8E-02	1.4E-01	1.2E-01	4.4E-01
MW-3006 TO MW-2022**	4.0E-03	1.3E-01	1.4E-01	7.4E-02	8.0E-02
MW-2028 TO MW-2024**	1.9E-02	2.5E-02	2.4E-02	6.7E-02	6.8E-02

* To convert the velocity to units of ft/d, multiply by 3.28.

** Flow path in the deeper portion of the Burlington-Keokuk aquifer.

aquifer/jcd/jof

on the basis of contaminant distribution, suggests poor hydraulic communication.

7.2 Groundwater Velocities

7.2.1 Results

Determination of effective porosity from the tracer test data allows for the calculation of natural average linear groundwater velocities. The average linear velocity is determined using Darcy's law in the form:

$$V = \frac{Ki}{n}$$

(14)

where:

    v = average linear groundwater velocity
    K = hydraulic conductivity
    i = hydraulic gradient
   n = effective porosity (0.007 as determined from tracer tests)

Groundwater velocities were calculated for the five potential flow paths described above. These flow paths refer to the path that a molecule of water follows from point A to point B assuming an equivalent porous medium approach; they do not account for velocity anomalies due to free flow conditions (heterogeneities), or horizontal anisotropy (i.e. the calculation assumes a homogeneous isotropic flow media). Figure 7-1 shows the selected shallow flow paths and Figure 7-2 shows the deeper flow paths.
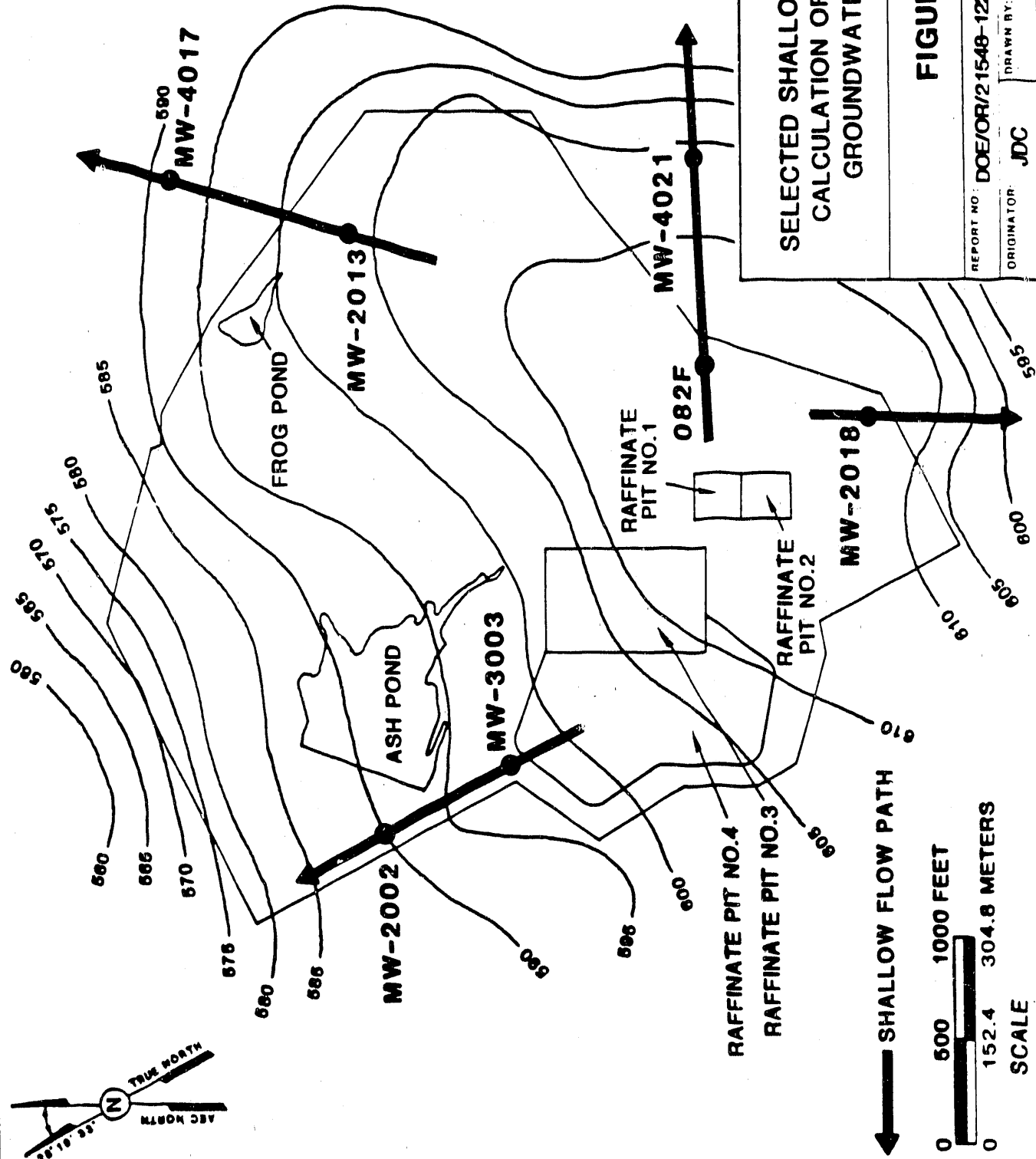
SELECTED SHALLOW FLOWPATHS FOR
CALCULATION OF AVERAGE LINEAR
GROUNDWATER VELOCITY

FIGURE 7-1

REPORT NO: DOE/OR/21548-122		DRAWING NO.: A/CP/009/0590
JDC	DRAWN BY: GLN	DATE: 5/90
ORIGINATOR:		
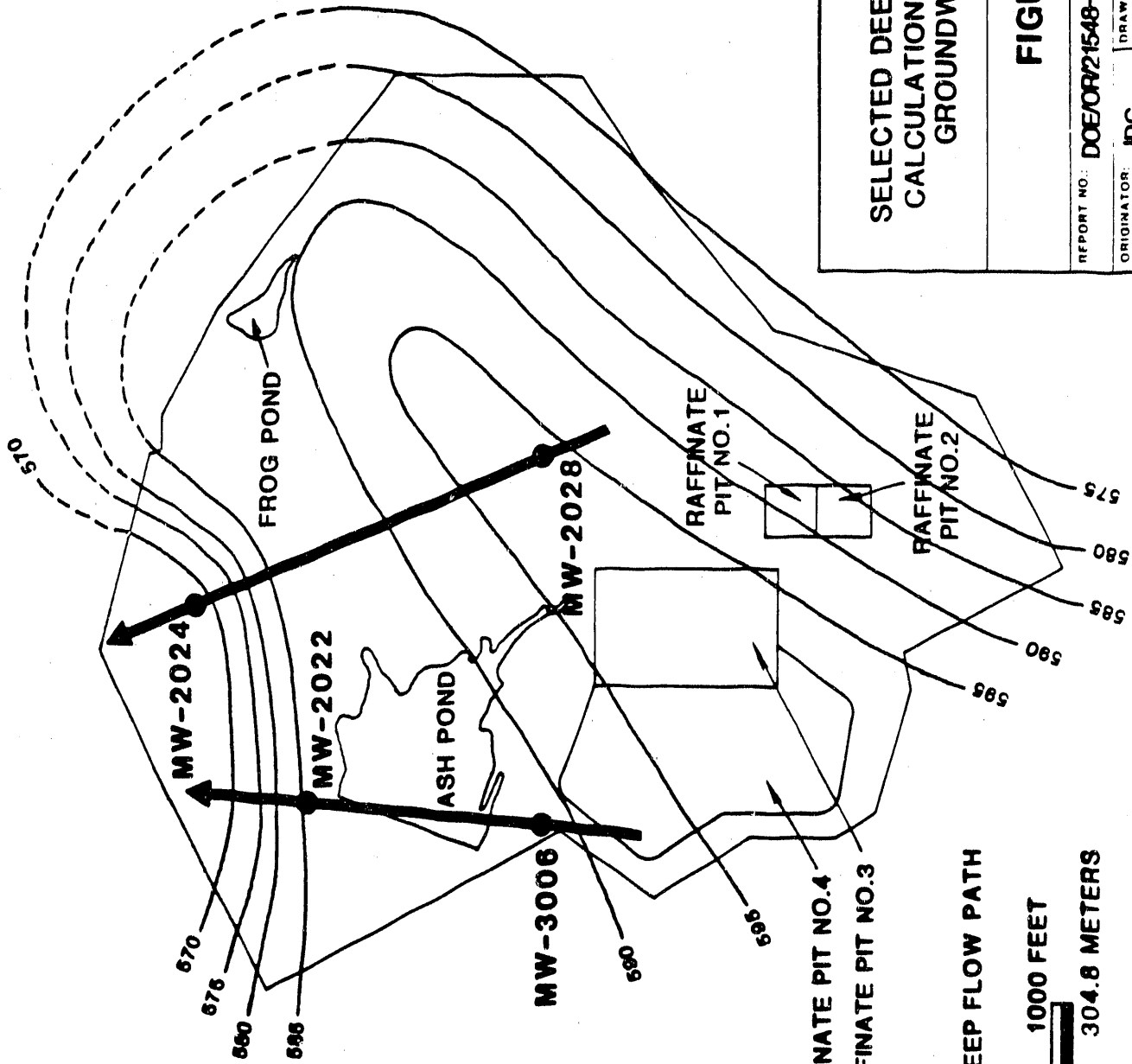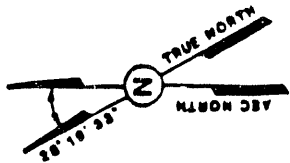
SELECTED DEEPER FLOWPATHS FOR
CALCULATION OF AVERAGE LINEAR
GROUNDWATER VELOCITY

FIGURE 7-2

Average hydraulic conductivities of wells along the selected flow
paths were used. Values of the hydraulic gradients and hydraulic
conductivities and the resulting velocities along each flow path
are presented in Table 7-1.

Using hydraulic conductivities determined by the Bouwer and
Rice method, average linear velocities ranged from a minimum of
0.022 m/day (0.072 ft/day) between OB2F and MW-4021 to a maximum
of 0.12 m/day (0.39 ft/day) between MW-2018 and MW-4022. Using
hydraulic conductivities determined by the Hvorslev method,
average linear velocities ranged from a minimum of 0.033 m/day
(0.11 ft/day) between OB2F and MW-4021 to a maximum of 0.44 m/day
(1.40 ft/day) between MW-2018 and MW-4022.

7.2.2 Discussion

To verify the values of average linear velocity presented in
Section 7.2.1 and the underlying assumption that Darcian diffuse
flow principles can be applied to assess contaminant transport, a
comparison of calculated travel times to observed contaminant
distribution can be made. Using the concentrations of nitrate
along the flow path from MW-3003 to MW-2002 as presented in the
Phase II Groundwater Quality Assessment for the WSCP/WSRP/WSVP
(MKF and JEG 1989a), a travel time of about 30 years can be used
to delineate the time since raffinate wastes were first
introduced into the holding pits. Seepage rates for the
raffinate pits (BNI 1986) and isopach thicknesses for the
overburden of 12 m (40 ft) were used to calculate a velocity and
travel time, assuming a hydraulic gradient of 1, and a porosity
of 0.36 (BNI 1987).

The calculated travel time for nitrate to reach the phreatic
surface is about 13.5 years, without taking into account initial

unsaturated flow which would conceivably lengthen travel time.
This leaves a balance of 16.5 years for contaminants to reach
their present distribution. The estimated travel time for flow
from the middle of Raffinate Pit 3, the approximate center (and
source) of the nitrate plume, to MW-2002, near the edge of the
plume, is about 21 years using average hydraulic conductivity
values obtained along the flow path between MW-3003 and MW-2002.
Combining the time required for nitrate to reach the phreatic
surface and the time required for the plume to reach its present
horizontal extent yields a total estimated travel time of about
35 years. While these values are admittedly only rough
estimates, the fact that they are fairly close corroborates the
calculated values for hydraulic conductivity (Section 6.1) and
average linear velocity (Section 7.2.1).

From Table 7-1 it can be seen that the calculated velocities
in the flow paths in the deeper portion of the Burlington· eokuk
are not substantially lower, as might be expected for flow in the
unweathered bedrock, than the velocities calculated for the
shallower flow paths. This is probably because observed
gradients between the deep wells imply the existence of a direct
lateral connection, which may not be the case. In fact flow
paths in the shallow and deep portions of the aquifer are
probably not linear as assumed in the derivation of horizontal
hydraulic gradients, but probably exhibit some degree of
tortuosity which would result in lower hydraulic gradients and
velocities. Therefore, the velocities presented in Section 7.2.1
represent maximum average linear velocities.

Conduit flow is considered to be limited to the highly
permeable portion of the weathered Burlington-Keokuk Formation.
No effort was made in this study to determine conduit flow
velocities. However, results of surface injection dye tracing

studies conducted by the Missouri Department of Natural Resources indicate that dye lost to conduit flow in the subsurface had flow velocities ranging from 0.4- to 0.7-m/min (1.5 to 2.2 ft/min) (MKF and JEG 1989b).

8 FINDINGS AND CONCLUSIONS

Findings and conclusions resulting from slug tests, pumping tests, and tracer tests performed to characterize the shallow Mississippian-Devonian aquifer in the vicinity of the WSS are presented below.

8.1 Findings

8.1.1 Slug Tests

o   The average hydraulic conductivity value for all wells tested was 7.4E-02 m/day as determined by the Hvorslev technique and 9.6E-02 m/day as determined by the Bouwer and Rice method.

o   Piezometer GT-58P yielded the maximum value for hydraulic conductivity, which was 3.9 m/day as determined by the Bouwer and Rice method.

o   Groundwater velocities calculated using hydraulic conductivity data obtained using the Hvorslev method yielded an average value of 1.8×10^{-1} m/day.

o   Groundwater velocities calculated using hydraulic conductivity data obtained using the Bouwer and Rice method yielded an average value of 1.1×10^{-1} m/day.

8.1.2 Pumping Tests

o   Mean transmissivity values were determined to be 2.34E-06 m^2/s (16.3 gpd/ft) for PW-1, 5.74E-06 m^2/s (39.9 gpd ft) for PW-2 and 2.23E-06-m^2/s (15.5 gpd ft) for PW-3.

o   The average storativity determined by pumping tests was 4.9E-04.

o   Hantush analysis yielded maximum apparent transmissivity tensor orientations of N72°W for PW-1, N10°W for PW-2, and N12°E for PW-3.

o   Comparison of maximum and minimum transmissivity values yielded anisotropy ratios of 2:1 for PW-1 and PW-3, and 3.5:1 for PW-2.

o   The radius of influence due to pumping is, generally, approximately 60 m (200 ft). However, along the line of OB1G, OB1H, and OB1I, the projected distance to zero drawdown was 275 m (900 ft).

o   Hydraulic conductivity values determined from pumping tests averaged 2.3E-02 m/day for PW-1, 4.9E-02 m/day for PW-2 and 3.1E-02 m/day for PW-3.

8.1.3 Tracer Tests

o   Effective porosities determined by tracer tests ranged from 0.002 to 0.015.

o   Dispersivity values determined by tracer tests ranged
from 8.8E-03 m for PW-3 (bromide) to 4.9E-02 m at PW-2
(chloride).

o   Breakthrough curves for tracers did not exhibit double
porosity effects.

8.2 Conclusions

Results of slug tests, pumping tests, and tracer tests
conducted at the Weldon Spring site (WSS) have yielded valuable
information about the shallow bedrock aquifer underlying the
site. The results presented herein represent a substantive body
of data which will be useful for remedial planning, assessing
aquifer restoration alternatives, feasibility assessments and/or
further monitoring programs, and groundwater modeling. With
these applications in mind, the following conclusions are
offered:

o   The aquifer of concern at the Weldon Spring site, is
composed of saturated rocks of the Burlington-Keokuk
Limestone which constitute the upper portion of the
Mississippian-Devonian aquifer. The aquifer of concern
is a heterogeneous anisotropic medium which can be
described in terms of diffuse Darcian flow overlain by
high porosity discrete flow zones and conduits.

o   Pumping and tracer tests did not intercept free flow
zones or conduits capable of supplying sustained pump
discharge yields in excess of approximately 1.5
liters/minute (0.4 gpm).

o   Slug tests performed on wells GT-58P, MW-4014, and

MW-4013 had high hydraulic conductivity values relative to the average which was 9.6E-02 m/day (Bouwer and Rice Method) for all wells tested. These values are considered to be representative of discrete flow in the fractured and weathered zones found in the upper Burlington-Keokuk Limestone and indicate heterogeneities within the upper Mississippian-Devonian aquifer. Aquifer heterogeneity in the horizontal plane is believed to be distributed randomly and is a function of fracture spacing, solution voids, and preglacial weathering phenomena. The relatively high hydraulic conductivities that may be encountered in deeper portions of the aquifer (e.g., MW-3006 with a hydraulic conductivity of 2.3E-01 m/day) are thought to be due to the presence of widely spaced fractures.

o   Piezometer GT-58P is a good location in which to consider an additional pump test because it has the highest hydraulic conductivity value of all wells tested. All indications suggest that flow at this location is discrete and, as such, sustained yields may be substantially in excess of rates required for the pumping tests addressed in this report (0.75-1.5 1 pm [0.2-0.4 gpm]).

o   Results of pumping tests indicate a primary lateral anisotropy and poor hydraulic communication between the pumped interval and deeper portions of the Burlington-Keokuk; thus, there is not likely to be significant upward leakage.

o   Calculated groundwater velocities and travel times
appear to be consistent with observed contaminant
distribution due to diffuse Darcian flow, although flow
paths may exhibit nonlinear aspects resulting in
significant variations in velocity.

o   Limited evidence of delayed yield such as that observed
near PW-1 may indicate double porosity effects.

o   Results of pumping tests, tracer tests, and slug tests
indicate limitations to an assessment of hydrologic
phenomena within the Burlington-Keokuk Limestone using
an equivalent porous medium approach. Additional
pumping tests of high hydraulic conductivity features
such as GT-58P may provide insight toward how
heterogeneous features influence the saturated zone.

9 REFERENCES

Allan, J.N., 1987. Letter to R. Nelson, U.S. Department of Energy, Weldon Spring Site Remedial Action Project. Subject: Falling Head Permedbility Tests. June 26.

Bear, J., 1972. Dynamics of Fluids in Porous Media. American Elsevier, New York, New York.

Bechtel National, Inc., 1984. Geologic Report Weldon Spring Raffinate Pits Site. DOE/OR/20722-6. November.

Bechtel National, Inc., 1986. Report on Water Balance Studies from 1983 to 1985 Weldon Spring Raffinate Pits. DOE/OR/20722-94. March.

Bechtel National, Inc., 1987. Hydrogeological Characterization Report for Weldon Spring Chemical Plant. DOE/OR/20722-137. July.

Berkeley Geosciences Associates, 1984. Characterization and Assessment for the Weldon Spring Quarry Low-Level Radioactive Waste Storage Site. DOE/OR/853. September.

BGA, see Berkeley Geosciences Associates

BNI, see Bechtel National, Inc.

Bouwer, H., 1989. The Bouwer and Rice Slug Test - An Update. Groundwater, Volume 27, No. 3 pp. 304-309.

Bouwer, H. and R.C. Rice, 1976. A Slug Test for Determining Hydraulic Conductivity of Unconfined Aquifers with Completely or Partially Penetrating Wells. Water Resources Research, Volume 12, No. 3. June.

Cooper, H.H., Jr. and C.E. Jacob, 1946. A Generalized Graphical Method for Evaluating Formation Constants and Summarizing Wellfield History. Transactions, American Geophysical Union. Volume 27, No. 4.

DA, see U.S. Department of the Army

Dean, T.J., 1983. Groundwater Tracing Project, Weldon Spring Area, St. Charles County, Missouri. Missouri Department of Natural Resources, Division of Geology and Land Survey. December.

Dean, T.J., 1984a. Groundwater Tracing Project, Weldon Spring Area, Interim Report, Part One. Missouri Department of Natural Resources, Division of Geology and Land Survey, April 24.

Dean, T.J., 1984b. Groundwater Tracing Project, Weldon Spring Area, Interim Report, Part Two. Missouri Department of Natural Resources, Division of Geology and Land Survey, November 2.

Dean, T.J., 1985. Groundwater Tracing Project, Weldon Spring Area, Interim Report, Part Three. Missouri Department of Natural Resources, Division of Geology and Land Survey, April 9.

Driscoll, F.G., 1986. Groundwater and Wells. Johnson Filtration Systems, Inc., St. Paul, Minnesota.

Eardley, A.J., 1951. Structural Geology of North America. Second Edition. Harper and Row.

Earth Scientists, Inc., 1989. Summary of Pumping Test Results and Evaluation; Wells 1, 2, and 3. Weldon Spring, Missouri. Subcontract No. 3589-SC-WP088.

ESI, see Earth Scientists, Inc.

Fetter, C.W. Jr., 1980. Applied Hydrology. Merrill Publishing Co. Columbus, Ohio.

Freeze, R.A. and J.A. Cherry, 1979. Groundwater. Prentice-Hall Inc. Englewood Cliffs, New Jersey.

Hantush, M.S. and R.G. Thomas, 1966. A Method for Analyzing a Drawdown Test in Anisotropic Aquifers. Water Resources Research. Volume 2, pp. 281-285.

Howe, W.B. and G.E. Heim, 1968. The Ferrelview Formation (Pleistocene) of Missouri, Report of Investigation No. 42. State of Missouri, Department of Business and Administration, Division of Geological Survey and Water Resources. Rolla, MO.

Hvorslev, M.J., 1951. Time Lag and Soil Permeability in Groundwater Observations. U.S. Army Corps of Engineers Waterways Experiment Station Bulletin No. 36, Vicksburg, Mississippi.

Javandel, I., C. Doughty, and C.F. Tsang, 1984. Groundwater Transport: Handbook of Mathematical Models. Water Resources Monograph Series 10. American Geophysical Union, Washington, D.C.

Kleeschulte, M.J. and L.F. Emmett, 1986. Compilation and Preliminary Interpretation of Hydrologic Data for the Weldon Spring Radioactive Waste Disposal Sites. U.S. Geological Survey Water Resources Investigations Report 85-4247.

Kleeschulte, M.J. and L.F. Emmett, 1987. Hydrology and Water Quality at the Weldon Spring Radioactive Waste Disposal Site, St. Charles County, Missouri. U.S. Geological Survey Water Resources Investigations Report 87-4169.

Kleeschulte, M.J. et al. 1986. Hydrologic Data for the Weldon Spring Radioactive Waste Disposal Site, St. Charles, Missouri, 1984-1986. U.S. Geologically Survey Open File Report 86-488.

Missouri Department of Natural Resources, 1989. First Annual Report on the Shallow Groundwater Investigations at Weldon Spring, Missouri.

MKF and JEG, see MK-Ferguson Company and Jacobs Engineering Group

MK-Ferguson Company and Jacobs Engineering Group, Inc., 1987. Determination of Maximum Earthquake for Weldon Spring Disposal Facility.

M-K Ferguson Company and Jacobs Engineering Group, Inc., 1988a. Radiologic Sampling Results and Needs for the Southeast Diversion Dike Interim Response Action. January.

M-K Ferguson Company and Jacobs Engineering Group, Inc., 1988b. Hydrogeologic Investigation Sampling Plan. DOE/OR/21548-020. November.

M-K Ferguson Company and Jacobs Engineering Group, Inc., 1989a. Phase II Groundwater Quality Assessment for the Weldon Spring Site Chemical Plant, Raffinate Pits and Surrounding Vicinity Properties, Revision B. DOE/OR/21548-078. August.

M-K Ferguson Company and Jacobs Engineering Group, Inc., 1989b. Draft: Remedial Investigation Report. Volume 1, Revision B. DOE/OR/21548-074. September.

M-K Ferguson Company and Jacobs Engineering Group, Inc., 1990. Draft: Suitability of the Weldon Spring Site for Potential Location of a Disposal Facility, Revision A. DOE/OR/21548-102. January.

MK-Ferguson Company and Jacobs Engineering Group, Inc., 1990b. Annual Site Environmental Monitoring Report 1989 for the Weldon Spring Site Remedial Action Project. DOE/OR/21548-129. May.

Oak Ridge National Laboratory, 1988. Work Plan for the Remedial Investigation/Feasibility Study-Environmental Impact Statement for the Weldon Spring Site. DOE/OR/21548-033. August.

ORNL, see Oak Ridge National Laboratory

Roberts, C.M. 1951. Preliminary Investigation of Groundwater Occurrences in the Weldon Spring Area, St. Charles County, Missouri. USGS. December.

UNC Geotech, 1988. Radiologic Characterization of the Weldon Spring, Missouri, Remedial Action Site. February.

U.S. Department of the Army, 1976. Assessment of the Weldon Spring Chemical Plant in St. Charles County, Missouri. March.

Whitfield, J.W., K.G. Brill, Jr., and W.J. Krummel, 1989. Geologic Map of the Weldon Spring 7 & 1/2" Quadrangle, St. Charles County, Missouri. OFM-89-252-GI. Missouri Department of Natural Resources, Division of Geology and Land Survey. Rolla, MO.

END

DATE FILMED

01/29/91